Electronic Control of Single-Molecule Dynamics

Andrew J. Mayne, Gérald Dujardin,* Geneviève Comtet, and Damien Riedel

Laboratoire de Photophysique Moléculaire, CNRS, UPR 3361, Bât. 210, Université Paris XI, 91405 Orsay, France

Received March 7, 2006

Contents

1. Introduction

The concept of "electronic control of single-molecule dynamics" on surfaces has appeared only recently. This is the result of a long maturing process that started in the 1960s when electronic spectroscopy of gas- and liquid-phase molecules became an important problem. Tremendous progress in surface science for preparing and characterizing clean and well-reconstructed surfaces was necessary. At the same time, there has been a growth in the understanding of the electronic interactions between the molecules and the surfaces, both experimentally and theoretically. Studying the electron control of molecular dynamics at the level of a single molecule became possible at the beginning of the 1990s with the advent of the scanning tunneling microscope (STM) as an atomic size source of electrons to electronically excite individual molecules. After an introduction to the historical background in part 2, the various electronic excitation processes whereby the tunneling electrons transfer energy to the molecule will be discussed in part 3. Part 4 is devoted to a review of recent examples of electronic control of single-molecule dynamics, ranging from bond-breaking such as dissociation and desorption to bond-making experiments where chemical reactions are induced molecule by molecule. The most recent example is that of the electronic control of a bistable molecule on a semiconducting surface. The STM manipulation experiments illustrate the ability to control a reversible movement of a single molecule. This achievement opens the door to a new field of research where a single functionalized molecule can be considered as a real molecular nanomachine, the electronic control being the ideal method to power and control its operation.

* To whom correspondence should be addressed: Phone: 33 1 6915 7713. Fax: 33 1 6915 6777. E-mail: gerald.dujardin@ppm.u-psud.fr.

2. Historical Evolution of the Electronic Control of Molecular Dynamics

Electronic control of molecular dynamics started with gas-phase[1] and liquid-phase[2] molecules in the 1960s when electronic spectroscopy became an important prerequisite for the development of a number of research fields ranging from plasma physics, photochemistry, and electrochemistry to atmospheric and interstellar chemistry. Molecular dynamics involved a large variety of processes, for example, fluorescence, change of configuration, dissociation,[3] ionization,[4] or chemical reaction.[3] Experimentally, electronic excitation was performed by photon absorption using lamps,[5] lasers,[3] or synchrotron radiation,[6] by electron impact,[7] or by electrochemical methods.[3] Spectroscopic information on the ground and excited electronic states of molecules in the gas and liquid phases forms the background knowledge issued from all these studies. A number of methods such as translational spectroscopy[8−10] provided not only spectroscopic information but moreover information on the molecular dynamics leading to dissociation of electronically or vibrationally excited molecular species. In that case, the excitation was performed by collisions at ∼1 keV[11] or inside an ion source.[12]

An important step in the electronic control of molecular dynamics has been the discovery of electronic nonradiative transitions (ENRTs).[13−15] The basic idea is that, due to the specific selection rules of photon excitation, the molecule can be excited into a nonstationary electronic state (Figure 1).[16,17] This nonstationary electronic excited state, as a coherent superposition of stationary states, will undergo an evolution over a short time that will drive the molecular dynamics.[13] In fact, this led to the first realization of coherent control of molecular dynamics. Further significant progress in the coherent control or quantum control of molecular dynamics has been achieved due to the development of femtosecond lasers.[18] This has enabled a considerable extension in the ability to control the molecular dynamics through a controlled preparation of coherent superpositions of electronic excited states.[18] Molecular ionization, dissociation, and orientation have been demonstrated by such quantum control experiments.

In the meantime, as these studies on the electronic control of molecular dynamics in the gas and liquid phases were

10.1021/cr050177h CCC: $59.00 © 2006 American Chemical Society
Published on Web 09/21/2006

Andrew J. Mayne received his B.A. in chemistry at New College, Oxford University, in 1990. This included an M.A. project on the two-photon spectroscopy in pentacoordinated uranyl compounds in the group of Prof. R. G. Denning. His postgraduate work in materials science at Oxford University was on the subject of the adsorption of small organic molecules on semiconductor surfaces using the scanning tunneling microscope, under the supervision of Profs. H. A. O. Hill and G. A. D. Briggs, for which he obtained his D.Phil. in 1994. He then moved to France, where he carried out his postdoctoral research with Gérald Dujardin at the Laboratoire de Photophysique Moléculaire (LPPM) at the University of Paris XI, in Orsay. The research focused on the room temperature (RT) STM manipulation of single atoms on semiconductor surfaces. In 1997, he joined the CNRS as a Chargé de Recherche to work with Gérald Dujardin, and his research covers the adsorption and manipulation with the RT STM of organic molecules on semiconducting and insulating surfaces, in particular those with a wide gap (SiC, diamond). He is equally involved in two projects concerning the fluorescence of individual nanoparticles under the STM tip and manipulation studies combining the STM with a laser.

Gérald Dujardin received his degree in physics from the Ecole Normale Supérieure (ENS), Cachan, France, in 1974. He obtained his Ph.D. at the University of Paris VI in 1978 for his work on "Stimulated emission from dye lasers: frequency locking and superfluorescence" under the supervision of Y. Meyer. This was followed by a state thesis in 1982 on "Non radiative electronic transitions of isolated molecular cations" under the supervision of S. Leach. He then worked on desorption induced by electronic transitions (DIET) by using synchrotron radiation. He started work on "Manipulation of individual atoms and molecules with the STM" at IBM (Yorktown, NY) in 1991 with Phaedon Avouris. Over the past 15 years, he has developed a team in Orsay which has acquired experience in atomic and molecular manipulation on semiconductor surfaces using the STM (Si, Ge, SiC, InSb, and diamond). He is presently Directeur de Recherche at the CNRS. His current research interests are focused on molecular nanomachines and their electronic control.

Geneviève Comtet received her degree in physics from the ENS, Sèvres, Paris, in 1974. Her Ph.D. (1977) and a state thesis (1982) on the predissociation and dissociation by the collisions of molecular ions was carried out at the Laboratoire des Collisions Atomiques et Moléculaires (LCAM) at the University of Paris XI, Orsay, under the supervision of P. Fournier. After a sabbatical year at the University of California at Los Angeles with Prof. El-Sayed and then with Prof. H. Bryant at Los Alamos National Laboratory, she returned to France to work on a project to create a source of polarized electrons with Roger Azria (LCAM) and also studied doubly charged ions with P. Fournier (LST). In 1989, she took the opportunity to study the adsorption of molecules on metallic surfaces using the synchrotron radiation facility at LURE in Orsay with J. Lecante. This led to her joining the group of Dr. Dujardin in 1992. Since then, her research has focused on the photoinduced processes in adsorbed molecules on semiconductor surfaces. She is responsible for projects on the fluorescence of individual nanoparticles under the STM tip and on the atomic force microscope (AFM).

Damien Riedel received his B.Sc. in physics from the University of Besançon. His M.Sc. work in optics and electronics was on speckle interferometry using a scanning near-field optical microscope in the Laboratoire d'Optique P. M. Duffieux. He obtained his Ph.D. in physics in 1998 under the supervision of Prof. M. C. Castex from the University of Paris XIII, where his postgraduate work in laser physics and surface science concerned the vacuum ultraviolet laser interaction with polymer surfaces and fluorescence spectroscopy. He then joined the group of Prof. R. E. Palmer in Birmingham, U.K., on a postdoctoral Marie-Curie Fellowship. In the Nanoscale Physics Laboratory, he worked on an ultra-short-pulse laser created by high-order harmonic generation in rare gases. He developed applications on surface photodesorption experiments and room temperature STM combined with a laser. In 2001, he joined the CNRS to work with Dr. Gérald Dujardin, and his research deals with molecular electronics and molecular manipulation via highly localized electronic excitation with a low-temperature STM on semiconductors. He is developing projects that combine a laser and an STM and involve collection of fluorescence on the low-temperature STM.

developed, researchers started being interested in molecules adsorbed on surfaces. The reasons for somewhat delaying the studies on surfaces as compared to those in the gas phase or liquid phase are essentially experimental. It was necessary to wait for the tremendous experimental progress in surface science that occurred in the two decades from 1960 to 1980 for preparing and characterizing clean and well-reconstructed metallic, semiconductor, and more recently insulator surfaces. Fundamentally, it has taken time to understand the electronic

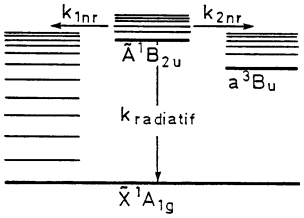

Figure 1. Schematic showing the electronic level manifolds of the benzene molecule. The state $\tilde{A}^1B_{2u}$ is coupled nonradiatively to the two vibrational-level continua of the X^1A_{1g} and a^3B_{1u} states. This diagram is based on the work presented in refs 13 and 17. For other examples of nonradiative transitions, see refs 14 and 15.

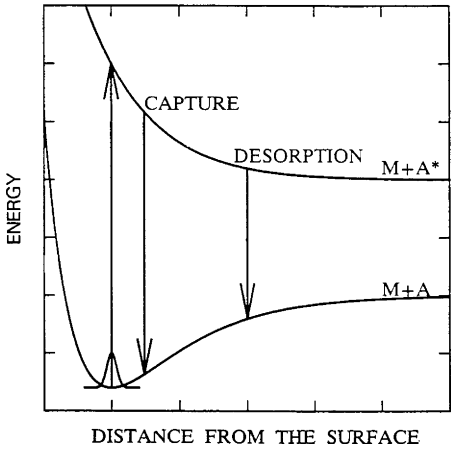

Figure 2. Schematic potential energy curves illustrating stimulated desorption by the Menzel−Gomer−Redhead model. A Franck−Condon transition from the ground state takes the system to a repulsive excited state. Quenching of the adsorbate excitation is assumed to return the system to a replica of the ground-state curve. Quenching can lead to either capture or desorption depending on where the quenching transition occurs. Reproduced with permission from ref 22. Copyright 1989 American Institute of Physics.

interactions between the molecules and the surfaces, from both an experimental and a theoretical point of view. Nevertheless, as early as 1964,[19,20] desorption from adsorbed molecules on surfaces induced by electronic excitation started to be investigated, motivated at that time mainly by the need to improve the technology of ion gauges for measuring ultra-high-vacuum pressures. This was the starting point of the so-called DIET (desorption induced by electronic transitions) studies,[21,22] whose impact has been continuously growing over the past 40 years. The DIET process is illustrated[22] in Figure 2, where stimulated desorption occurs according to the Menzel−Gomer−Redhead model.[19,20] Here, a Franck−Condon transition from the ground state takes the system to a repulsive excited state. Quenching of the adsorbate excitation is assumed to return the system to a replica of the ground-state curve. Quenching can lead to either capture or desorption depending on where the quenching transition occurs. Not only has desorption been considered, but all kinds of molecular dynamics including dissociation, ionization, diffusion, and chemical reactions have been explored. Various excitation processes have been used to induce and study the electronic excitation of adsorbed molecules on surfaces: synchrotron radiation,[23,24] electron impact,[25] ion impact,[26] and lasers.[27] Thus, DIET has now acquired a very mature status.[28] There are several fundamental differences between DIET processes at surfaces and the electronic control of molecular dynamics in the gas or liquid phases. The major difference is the efficient dissipation of molecular energy, both electronic and vibrational, on a surface. This

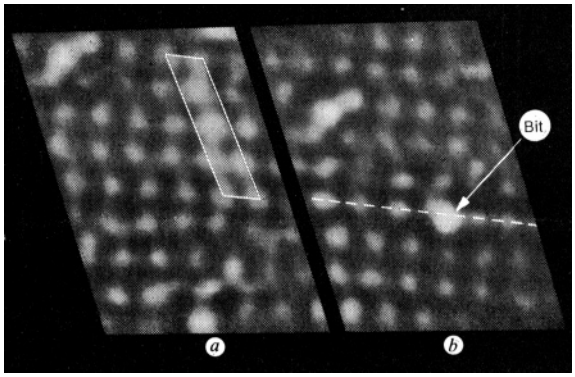

Figure 3. Tunneling images of a reconstructed (111) germanium surface covering a 50 × 65 Å^2 region. (a) Surface before modification. A single unit cell of the c(2×8) reconstruction is highlighted, and a naturally occurring defect in the upper left-hand corner serves as a registration mark. (b) Same region after the surface modification. The displayed region is slightly translated due to the thermal drift in the tunneling microscope. The new bright spot near the center of the picture is the impressed bit. Reproduced with permission from *Nature* (http://www.nature.com), ref 31. Copyright 1987 Nature Publishing Group.

results in (i) relatively low efficiencies of DIET processes,[19] (ii) molecular dynamics at surfaces occurring in the relaxed electronic state,[19] and (iii) coherent control of molecular dynamics being difficult on surfaces.[29]

Soon after the discovery, in 1990, that the tip of an STM could be used to laterally move individual atoms and molecules in a controlled manner across a surface,[30] it was realized that the STM tip could also be used as an atomic size source of electrons for local electronic excitation. This had been performed on the Ge(111)-c(2×8) surface.[31] Here, −4 V pulses deposited single atoms on the surface from the tip (Figure 3). This result is important historically because it was the first demonstration of a controlled vertical manipulation and the authors were the first to suggest an application in nanotechnology. Other demonstrations of the new capabilities of the STM included the desorption of hydrogen from a hydrogenated Si(111)-7×7 surface[32] and the transfer of individual atoms between a surface and a tip by the application of voltage pulses.[33] The first molecular dynamics induced by electronic excitation with the STM has been the dissociation of decaborane molecules adsorbed on a Si(111)-7×7 surface.[34] The dissociation was monitored through the observation of molecular fragments on the surface. A threshold voltage around +4 V indicated that the excitation mechanism was indeed an electronic excitation. In the following paragraphs, the basic principles of these electronic processes induced with the STM tip will be discussed in more detail. The most recent examples of the electronic control of molecular dynamics using these STM methods will be examined.

3. Electronic Excitation Processes with the STM

We will define "electronic excitation" as a process where the dynamics, the structure, and/or the lifetime of the electronic excited state play a role in the STM manipulation process even though the system rapidly relaxes to its ground electronic state. The underlying process, fundamental to electronic excitation of an adsorbed atom or molecule, is that the transport of electrons between the tip and the surface must dissipate some energy through inelastic electronic coupling. This will manifest itself experimentally by the

observation of a clear electronic resonance or electronic threshold[34−36] in the manipulation cross section variation as a function of the surface voltage.

In most cases, the STM is used for both the imaging and manipulation of an adsorbate. As such, it is important that imaging does not in itself induce any modification. Therefore, it may be useful to give the typical imaging and manipulation conditions. In a typical STM scan (20×20 nm^2, 100 nm s^{-1}, 400×400 pixels), a single molecule (0.3×0.3 nm^2) receives a dose of 10^8 electrons at 1 nA. Most atom or molecular manipulation processes have yields of between 10^{-11} and 10^{-6} events per electron; that is, between 10^6 and 10^{11} electrons are required. Thus, for processes with a high yield, all molecules could react if the voltage is above an excitation threshold. So for experiments on semiconductor surfaces, it is necessary to use low voltages and low currents to image the surface if one wants to avoid manipulation of any adsorbed molecules. Typically, the voltage and current are ± 2 V and less than 0.5 nA, respectively, while manipulation is carried out for voltages greater than ± 2 V and currents anywhere between 0.2 and 30 nA. For experiments on metal surfaces, imaging occurs at low voltages (100 mV) while currents are less than 1 nA and may even be only a few picoamperes. The manipulation conditions depend on the effect desired; vibrational manipulation requires a low voltage, whereas atom displacement or desorption requires higher voltages. It is clear that manipulation is much more dependent on the voltage applied than the current.

Consider the situation where an atom or a molecule is adsorbed on a surface. The atom or molecule will have unoccupied states that lie above the Fermi level of the surface. Some of these unoccupied states will be above the vacuum level (of the surface), while others will be below. The states lying above the vacuum level are accessible with far-field techniques such as electron impact scattering. If the STM tip is used to induce electronic excitation by injecting electrons into these antibonding orbitals, access to all the antibonding states is possible, even those that lie below the vacuum level of the surface. It should be pointed out that lasers and other photon sources can be used to inject electrons into the LUMO of an adsorbate. Indeed, this has been demonstrated in a recent experiment by Ho and co-workers where irradiating an Ag tip with visible wavelength photons induced electron transfer to a metal porphyrin molecule adsorbed on a surface under the tip.[37] However, these photon or electron sources produce vast amounts of secondary electrons, and secondary electron processes are not necessarily desirable in that they complicate greatly the interpretation of the manipulation events. Thus, if they can be avoided or at least reduced, this will help in an initial understanding of the manipulation events. This is possible with the STM. In general, the probability and efficiency of the electronic transition will be determined by the overlap and coupling of the tip and molecular wave functions across the tunnel barrier. The possible means of excitation are grouped into three categories, electron attachment, electron transition, and electron−hole pair attachment, which are schematically shown in Figure 4.

If we compare electronic excitation with vibrational excitation or direct contact (between the STM tip and the molecule), electronic excitation has several advantages if one wants to induce dynamical processes; for example, electronic excitation can induce fluorescence, whereas vibrational excitation cannot. First, electronic excitation should enable

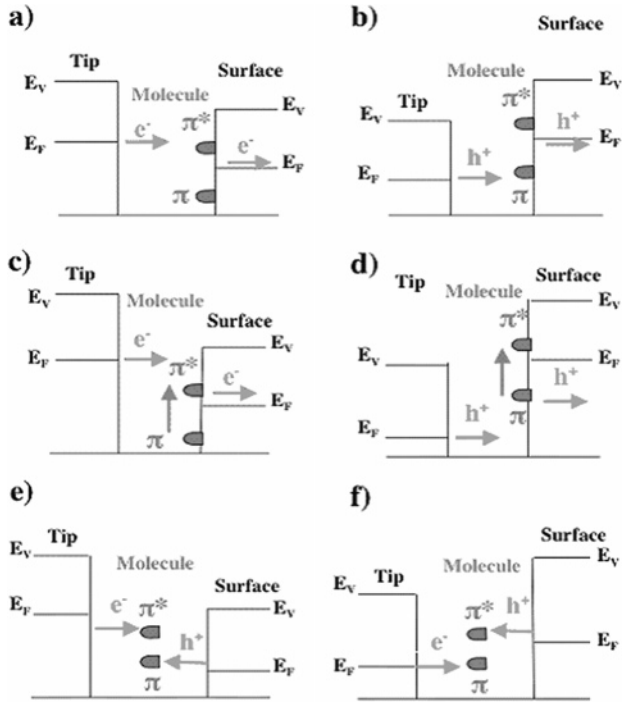

Figure 4. Schematics of the electronic excitation processes of a molecule under the STM tip: (a) electron attachment, $V_S > 0$; (b) hole attachment, $V_S < 0$; (c) electronic transition, $V_S > 0$; (d) electronic transition, $V_S < 0$; (e) electron−hole pair attachment, $V_S > 0$; (f) electron−hole pair attachment, $V_S < 0$.

the molecule to be excited into far-from-equilibrium conformations, resulting in very rapid, efficient, and more easily controllable molecular dynamic processes. Second, the transfer of energy should be more rapid. Third, electronic excitation can be used to activate different molecular functions. These can be different in nature; for example, an electronic function might involve a change in transport properties of the molecule. A mechanical function might involve a change in configuration, and an optical function might induce fluorescence from the molecule. Last, quantum control of isolated molecules has been demonstrated in the gas phase using the laser to induce electronic excitation.[38] However, control is achieved by tuning the coherence time between the excitation and the final state. Coherent control of a molecule can be achieved using femtosecond lasers.[27] However, coherent control can also be achieved by fabricating a nonstationary state through specific selection rules without short-pulse excitation.[13] This has been known for a long time in gas-phase experiments. This nonstationary state can be described as a superposition of real stationary states as illustrated in Figure 1. It is through this method that we might be able to initiate a coherent control with the STM, though it remains to be seen if this is possible on a surface using tunnel electrons from the STM tip via electronic excitation.

Using the STM tip to induce the electronic excitation offers another advantage. That is, the STM can determine the precise position of each atom or defect. This leads us to consider also some of the difficulties that can be encountered when using the STM. For example, the electronic or chemical properties of an individual molecule can be strongly modified by the presence of a given atom in its neighborhood.[39] The difficulty here is that each atom or molecule on the surface may behave differently due to a different atomic-scale environment. For example, the switching probability of the

biphenyl molecule adsorbed on the Si(100)-2×1 surface[36] was dependent on the proximity of neighboring molecules and on whether the underlying silicon dimers were buckled. Quantitative measurements of the molecular properties may then become a real problem. Furthermore, the precise identification of the electronic processes under the STM tip can be made difficult by the lack of knowledge of the electronic structure, on the atomic scale, of occupied and unoccupied states of adsorbed atoms and molecules. Another complication is that the presence of the STM tip close to the surface can modify the atomic and electronic structure of the adsorbed atom or molecule, either through direct contact between the STM tip and the surface or through the relatively strong electric field between the tip and the surface.[40] Finally, it should be noted that both the electronic excitation and the probing of the molecular dynamics are achieved with the same tool, i.e., the STM tip.[36] This makes the realization of a spatial experiment where one excites a molecule at one position and measures the result at another position very difficult. The coherence process of electron tunneling through the barrier between the tip and the surface has never been tested. Furthermore, the measurements do not take place on the same time scale as the excitation. This is in stark contrast to the temporal control and coherence that can be achieved in a pump−probe experiment using two different lasers to excite and probe the molecular dynamics in the gas phase.

A final subject needs to be raised: the role of the tip in manipulation processes. During manipulation, the process of injecting electrons from the tip should be independent of the tip. However, on semiconductor surfaces, the electric field present in the tunnel junction can induce band-bending, and this is very dependent on the structure and shape of the tip.[40−43] Several experiments will be discussed in section 3.5 where the electric field is the primary agent in the manipulation process.

3.1. Electron (Hole) Attachment

Electrons from the STM tip can be attached temporally to an unoccupied orbital of an adsorbed atom or molecule, producing a negatively charged species (Figure 4a). Such a process is the surface analogue of a negative ion resonance in the gas phase.[44] Using the STM, this manipulation requires a positive voltage on the surface with respect to the tip, $V_S > 0$. The electron attachment process has been considered to explain a variety of manipulation experiments.

The most widely studied has been the desorption of individual hydrogen atoms from the fully hydrogenated Si(100)[45−52] and partially hydrogenated Ge(111)[53−56] surfaces through the attachment of electrons to the σ^*(Si−H) and σ^*-(Ge−H) antibonding orbitals, respectively. The results from the early studies on the desorption of hydrogen from silicon showed the presence of another desorption regime with a threshold around 6.5 eV (Figure 5). This high-energy regime will be discussed in the next section as it corresponds to a direct $\sigma-\sigma^*$ excitation of the Si−H bond.[57,58] In the low-voltage regime, the desorption yield was found to be several orders of magnitude lower and showed a distinct power law behavior as a function of the current for a given applied voltage. Between 2 and 4 V, the yield increased by more than a factor of 10 as the current was increased from 1 to 3 nA (Figure 6). The current dependence was explained by the desorption resulting from an electron attachment to the σ^*(Si−H) orbital via vibrational heating of the Si−H bond

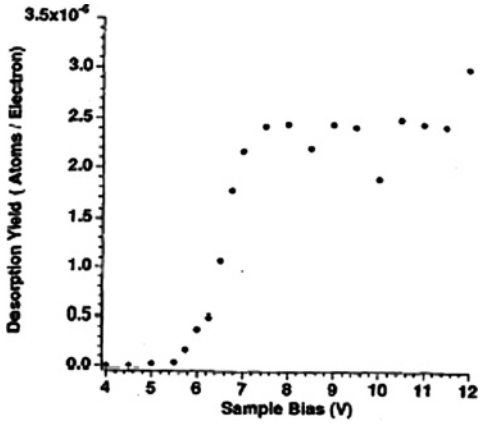

Figure 5. STM tip-induced desorption of hydrogen atoms from the Si(100)-2×1 surface. H atom desorption yield as a function of the sample bias voltage. The tunnel current was 0.01 nA. The sample was As-doped, 5×10^{-3} Ω cm. Reproduced with permission from ref 57. Copyright 1996 Elsevier.

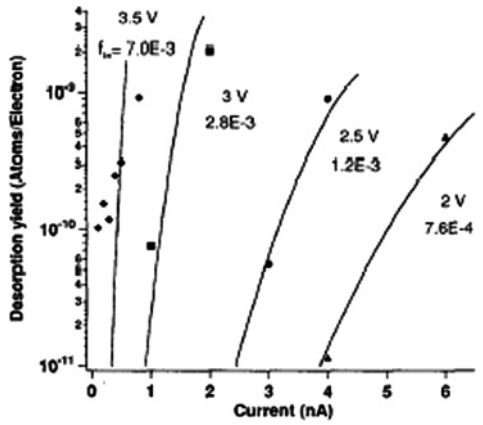

Figure 6. H atom desorption yields at incident electron energies (bias voltage) below the electronic transition threshold (see Figure 5). The curves shown are the predictions of the truncated harmonic oscillator model of multiple vibrational excitation. The inelastic fractions f_{in} obtained from fitting to the data are given next to the curves. Reproduced with permission from ref 57. Copyright 1996 Elsevier.

where 10 or more electrons were needed—each electron giving only a small fraction of its energy to the Si−H bond (1 quantum).[45−50] However, the resonant character of the process has not been clearly established.

Later studies on Si(100):H were carried out over a larger current range (1−10 nA). The desorption yield showed only a weak current dependence for both n-type and p-type samples and for both the stationary and line-scan modes (Figure 7). The desorption yield had the same absolute value as that found in previous studies, but only a very small dependence of the desorption yield on the current was found where only two electrons are required to break the Si−H bond.[51] Further studies indicated that the tip plays an important role which is hard to quantify.[52] It was observed that the lines drawn by the tip were segmented such that from time to time no hydrogen was removed, suggesting that the tip had "on" and "off" modes (Figure 8). This could be due to the fact that a large number of hydrogen atoms are removed in a short amount of time so the tip is easily passivated, which can change the efficiency of the desorption process.

Two models of electronic excitation via vibrational heating exist; one is called coherent excitation[59] and the other

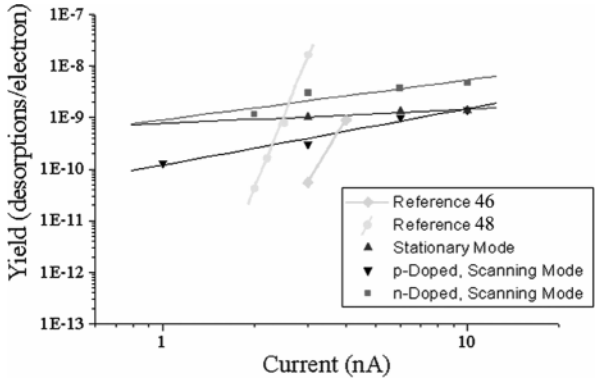

Figure 7. Desorption yield as a function of the tunneling current in stationary mode for p-type samples (up-triangles) and in scanning mode for p-type samples (down-triangles) and n-type samples (squares). The solid lines are the corresponding least-squares fit to a power law, I^a. The exponents are $a = 0.3 \pm 0.1$, 1.3 ± 0.3, and 0.8 ± 0.3, respectively. The values of the yield from previous studies as a function of the tunneling current (ref 46 (circles) and ref 48 (diamonds)) and the respective least-squares fit to a power law, I^a. The exponents are $a = 15$ and $a = 10$, respectively. Reproduced with permission from ref 51 (http://link.aps.org/abstract/PRB/v68/p035303). Copyright 2003 American Physical Society.

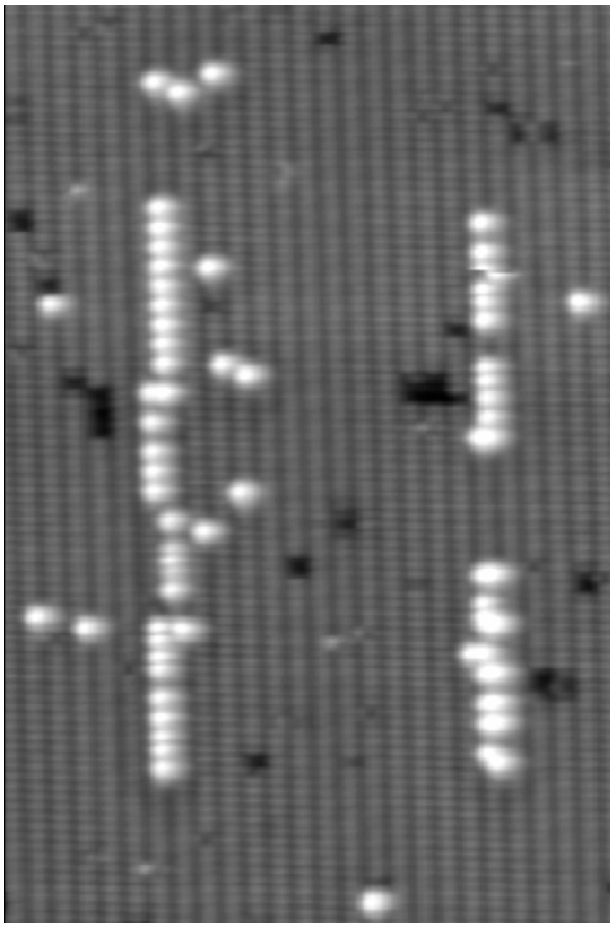

Figure 8. STM topography (50×25 nm^2) of a hydrogenated Si(100)-2×1 surface showing two lines of silicon dangling bonds (DBs) produced by extracting the hydrogen atoms with the STM tip. Imaging conditions were −1.5 V and 0.5 nA for the topography and the hydrogen extraction at +2.5 V and 6 nA at a scan speed of 80 nm/s. Kinks in the DB lines are mainly due to misalignment of the tip trajectory with the dimer rows. The right-hand line shows both a Peierls distortion and a section where the tip is inactive.

incoherent.[60] These are analogous to the DIET and DIMET processes, respectively. In both cases, the electron attaches

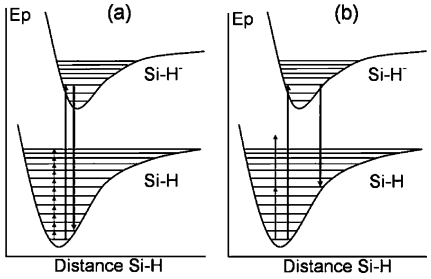

Figure 9. Diagrams showing the two different models for the desorption of hydrogen, from a hydrogenated Si(100)-2×1 surface, induced by the tunnel electrons. In both cases, the first step is a resonant Franck−Condon excitation where the arrival of the electron creates an excited Si−H$^-$ species. (a) Vibrational heating mechanism. Each electron transfers one quantum to the Si−H bond during the relaxation process. (b) Derivative of the coherent model. Each electron transfers a large proportion of its energy to the Si−H bond during the relaxation process.

to the σ^*(Si−H) orbital, forming a negative ion resonance, and then as the electron leaves (to the surface), it transfers some part of its energy to the Si−H bond. In the first model, excitation produces a coherent superposition of vibrational states and in the second an incoherent superposition of vibrational states. Thus, in the "coherent" model, several quanta are transferred, thereby allowing the electron to climb the vibrational ladder several levels at a time, whereas in the "incoherent" or vibrational heating model, the electron transfers only one quantum, thereby climbing the vibrational ladder only one level at a time. The coherent mechanism had been shown to dominate at low tunnel currents where the average time between successive electron tunneling events is longer than the vibrational lifetime. The more recent results[52,53] are more compatible with the coherent model for exciting the Si−H bond as proposed by Persson and Palmer,[60] since only two electrons are needed to induce hydrogen desorption. This casts doubt over the validity of the incoherent vibrational heating mechanism as the description of the hydrogen extraction process; at 10 nA, the time between tunnel events is around 2 ps, which is much shorter than the vibrational lifetime of the excited state of the Si−H bond (10 ns).[61] An illustration of the two models based on the literature[59,60] is given in Figure 9.[62]

There are a number of practical complications related to the early results by Shen et al.[46] The major problem with the results produced by Lyding, Avouris, Stokbro, and others[45−50] was the lack of precision due to the line-scan method used. It was difficult to determine the exact number of electrons involved since the tip is scanned over the surface. The whole line receives a certain dose of electrons, so depending on the speed, several electrons can interact with a single hydrogen atom or between hydrogen atoms, which renders an understanding of the physical process of desorption more difficult. This means that the inelastic coupling will vary from site to site. As a consequence, it seems hard to justify the mechanism given the uncertainties and especially the lack of experimental data points.

In studies of the desorption of hydrogen from germanium, individual hydrogen atoms are adsorbed on the Ge rest atom sites and at low exposures are isolated from each other. This is shown in Figure 10, where three hydrogen atoms are adsorbed on the Ge surface.[53] The hydrogen atoms show up as characteristic triangle and square sites where the three and four nearest-neighbor adatoms have more electron density than usual due to a transfer of charge. In addition to

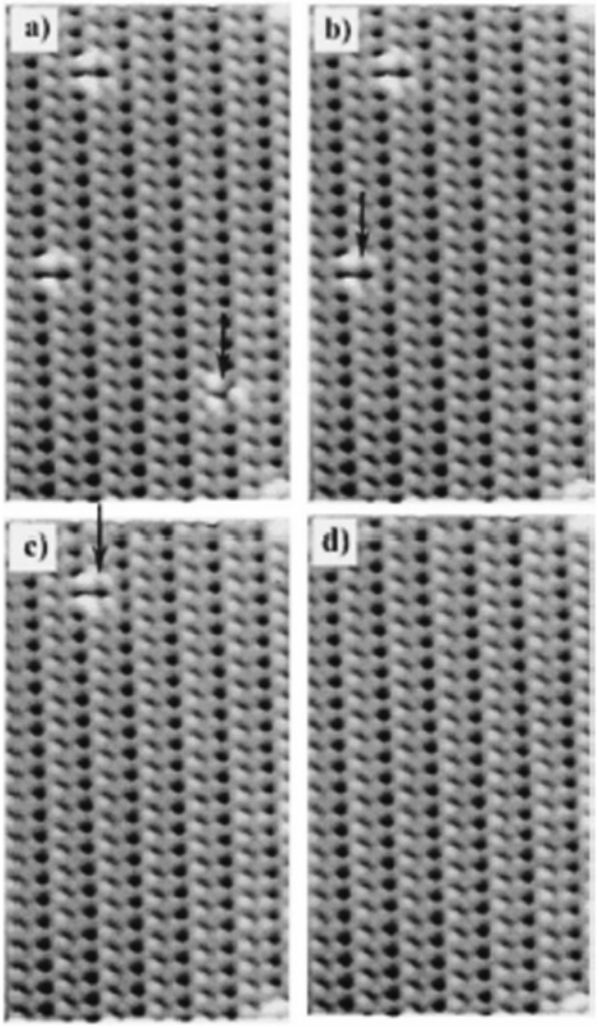

Figure 10. Sequence of four consecutive STM topographic images (45×185 Å^2) of a Ge(111)-c(2×8) surface. The imaging conditions were −1 V and 1 nA in each case. The first contains three hydrogen atoms (two square sites and one triangular site) and a defect in both the top-right and bottom-right corners. A single pulse was applied to the first H as indicated by the arrow, and the resulting extraction can be seen in the subsequent image. Pulses were then applied to the other two hydrogen atoms in turn. Reproduced with permission from ref 53 (http://link.aps.org/abstract/PRB/v63/p081305). Copyright 2001 American Physical Society.

the adsorption of hydrogen on the rest atom sites (triangle and square), a new site, called a zip site, has been observed which was the result of a local rearrangement of the c(2×8) structure.[54] These confirmed the earlier STM study by Klistner and Nelson[63] showing that the adsorption of hydrogen takes place on the rest atom sites and not on the adatom sites, where they suggested that the adsorption of hydrogen causes a very local transfer of charge from the rest atom to the nearest-neighbor adatoms. The hydrogen atoms are removed one by one with the STM tip using a voltage pulse.[55] As shown in Figure 11, it was observed that the desorption yield increased for sample voltages above 4 eV.[53,56] During each voltage pulse, the tip was retracted by 2−20 Å, giving a measurable current of between 10 and 0.2 nA. For all voltages, the yield at each point in Figure 11b is the average of the different measured $I\tau$ values. Thus, the desorption yield was clearly independent of the tunnel current and of the tip−surface distance. This suggested that a single-electron excitation was taking place not involving multivi-

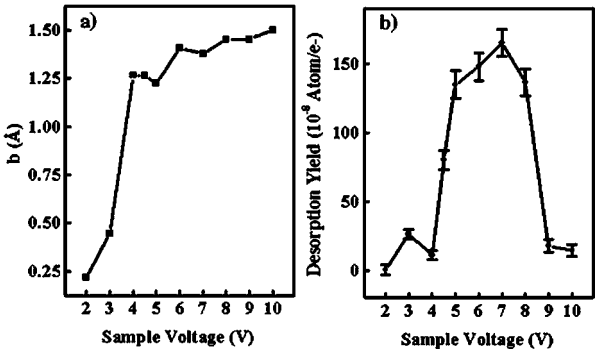

Figure 11. Desorption of H atoms adsorbed on a Ge(111)-c(2×8) surface. In (a), the spread distance b is shown as a function of the applied bias V_S. In (b) is shown the desorption yield Y as a function of the applied bias V_S. Reproduced with permission from ref 53 (http://link.aps.org/abstract/PRB/v63/p081305). Copyright 2001 American Physical Society.

brational processes (unlike silicon) and that the electric field could be neglected. The electric field was estimated to be less than 0.3 V/Å. Furthermore, the Ge−H bond energy of 3.0 eV[64] is low enough that a single electron is sufficient to break the bond in the voltage range 3−10 V. For Ge−H, the known electronic excitation processes are resonant electron attachment of an electron in the σ^*(Ge−H) antibonding orbital (unoccupied) at 3.5 eV above the Fermi level[65] and the direct $\sigma-\sigma^*$(Ge−H) transition at 8.5 eV.[66] The most likely explanation of the increase in the yield above 4 eV is that of the attachment of tunnel electrons into the σ^* Ge−H orbital.

Similar processes have been considered to explain the STM tip-induced desorption and hopping of individual CO molecules from a Cu(111) surface.[35] Here, it was observed that individual CO molecules could be desorbed by applying a bias above a threshold of 2.4 V. The desorption yield per electron was found to be 2.7×10^{-11}. The desorption yield was determined from the distribution of the hopping rates at 2.7 V and 4.7 nA. The mean hopping rate as a function of tunnel current was linear, which suggested a single-electron process. Time-resolved two-photon photoemission (2PPE) experiments were performed on the ordered submonolayer $\sqrt{3}\times\sqrt{3}$ phase of CO. In this phase, all the CO molecules are in on-top sites.[67] The results indicated a $2\pi^*$ excited state with a lifetime of between 1 and 5 fs. The conclusion was that the hopping process was induced by a single electronic transition of a CO molecule from its ground state to an excited $V_{2\pi^*}$ state via the attachment of a tunneling electron into the CO $2\pi^*$ state (Figure 12).

Electron attachment using the STM tip has been used to manipulate adsorbed oxygen molecules on the Si(111)-7×7 surface.[68] The chemisorption of oxygen involves the transfer of an electron from the surface into the $2\pi^*$ orbital of the adsorbed species. This significantly weakens and elongates the O−O bond, thus lowering the energy of the $3\sigma^*$ orbital. Tight-binding calculations placed this orbital about 7 eV above the Fermi level.[69] Once an electron is captured in this σ^* state, two processes can occur, fragmentation of the molecule or desorption. This depends into which bond the energy is dissipated when the electron escapes. Vibrational excitation of the O−O bond leads to fragmentation, whereas de-excitation onto the repulsive part of the ground-state potential of the Si−O bond leads to molecular desorption. In the manipulation experiments[68] both modes were observed and depended on the local adsorption configuration. How-

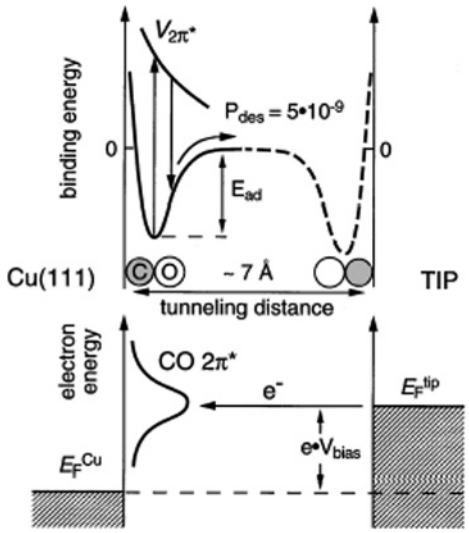

Figure 12. Top part: potential curve of the bound state of a CO molecule between the Cu(111) substrate (left) and the STM tip (right). A higher binding energy on the tip is assumed. Virtually no overlap between the two potential wells occurs. Additionally, the assumed potential curve V_{2pp} of the excited state is shown. The desorption process according to the MGR model is indicated with arrows. It has a yield per excitation of $P_{des} = 5 \times 10^{-9}$. Bottom part: At positive sample bias V_{bias}, tunneling electrons from the STM tip (right) can transiently occupy states of the sample between E_F and $e - V_{bias}$. Thus, at 2.4 V bias the electrons start tunneling into the 2pp state. Reproduced with permission from ref 35 (http://link.aps.org/abstract/PRL/v80/p2004). Copyright 1998 American Physical Society.

ever, the interpretation of the nature of the adsorbed oxygen species is not clear. There have been a number of experimental studies using the STM,[70−73] synchrotron radiation[24,74,75] and Cs^+ ion scattering,[76] as well as theoretical studies,[77,78] which illustrates that it is a challenge to distinguish between molecular adsorption and dissociation even with a multitude of different surface-sensitive techniques, especially at low coverages. The most recent experiment and calculations suggest that there is no molecular species at room temperature at very low coverage.[75,78] At low temperatures a molecular species may exist with a short lifetime.[79]

Another example of electron attachment is the tip-induced hopping of silicon adatoms on the Si(111)-7×7 surface at low temperatures as shown in Figure 13.[80] For an applied sample bias between 3 and 10 V, the hopping rate was found to be linear over 4 orders of magnitude in current. This indicates a one-electron process. The hopping yield was measured at 7.4×10^{-9} transfer per electron. A significantly lower yield was measured for 2.25 V and high currents (5−100 nA). This was explained in terms of an increase in the voltage drop between the surface adatoms and the bulk states with increasing current. Calculations had shown the existence of conduction-band surface resonances on the bare Si(111) surface between 3 and 8 eV above the Fermi level.[81] These correspond to the σ^* antibonding states of the Si adatoms. The results suggest that the dominant mechanism is the temporary attachment of the electrons from the tip to these resonances. Multiple vibrational excitations are believed not to occur due to the very short vibrational lifetime of the Si adatom as compared to the mean time between two consecutive electrons (tunneling current rate). The top of the bulk phonon band lies at 63 meV[82] and leads to an estimated lifetime of 10 fs. Since the mean time between tunneling

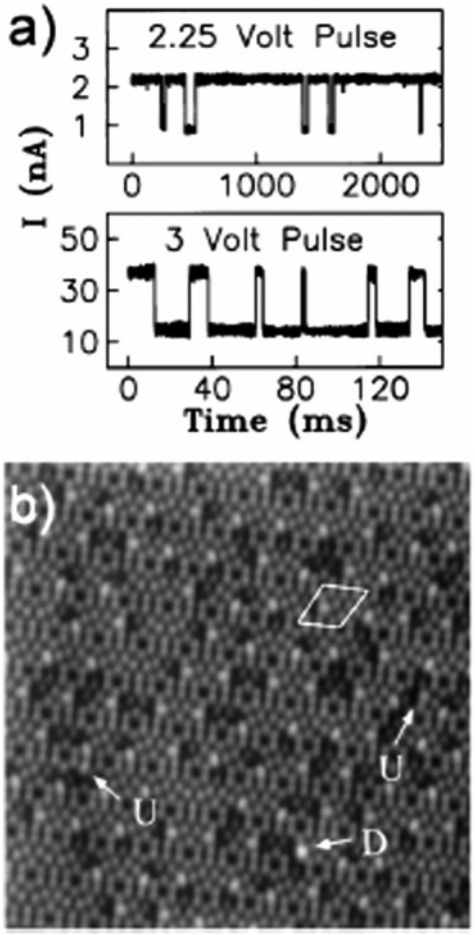

Figure 13. STM tip-induced hopping of silicon adatoms on the Si(111)-7×7 surface. (a) Current recorded at 2.25 and 3 V sample bias over a center adatom in the faulted half of a unit cell at 121 K. (b) STM image of the saturated surface at 52 K after a previous scan at 10 V showing an outline of the unit cell, a large number of transferred adatoms in the faulted halves, a double hop (labeled D), and two hops in the unfaulted half of the unit cell (labeled U). Reproduced with permission from ref 80 (http://link.aps.org/abstract/PRL/v79/p4397). Copyright 1997 American Physical Society.

events is 600 fs at 100 nA, the excitation process involves only one electron.

Electron attachment is not limited to the LUMO orbital. The attachment of electrons to highly excited unoccupied states of individual porphyrin molecules adsorbed on an ultrathin alumina film grown on a NiAl(110) surface has been shown to induce light emission.[83] Light emission from the porphyrin molecules occurs via two possible channels, either inelastic electron tunneling (IET) or molecular fluorescence. These two processes are illustrated schematically in Figure 14. A similar picture had been considered in a previous study of luminescence from quantum-well structures.[84] The IET process (process A in Figure 14) happens when the electrons from the tip tunnel inelastically into the LUMO of the molecule. This can be seen experimentally by the fact that the cutoff photon energy is less than the applied bias. On the other hand, fluorescence emission (process B in Figure 14) proceeds with electrons tunneling elastically into the molecule. This creates an electronically and vibrationally excited molecular state which has an anionic character. The molecule undergoes vibrational relaxation in the excited state and then a radiative transition to the lower electronic state. This radiative transition generates a tip plasmon which is then detected in the far field as a photon (this occurs for the

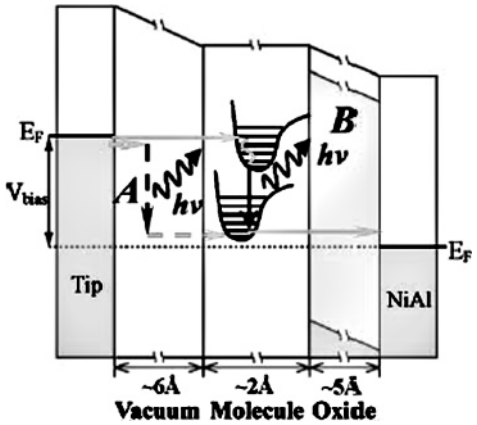

Figure 14. Diagram showing the two major processes contributing to STM-excited light emission from a molecule adsorbed on the oxidized NiAl surface. In process A, the IET channel, an electron inelastically tunnels from the Fermi level of the STM tip into an unoccupied molecular orbital with simultaneous excitation of a plasmon. In process B, the fluorescence channel, an electron tunnels into the higher unoccupied orbital of the molecule. The charged molecule then relaxes to a lower vibrational level of the same electronic level, with subsequent radiative (excitation of a plasmon) transition to the lower electronic level. The final step involves tunneling of this extra electron into the NiAl substrate. The plasmons are detected as photons in the far field. E_F is the Fermi energy and $h\nu$ the photon energy. Reproduced with permission from *Science* (http://www.aaas.org), ref 83. Copyright 2003 American Association for the Advancement of Science.

Ag tip but not the W tip). The extra electron in the lower electronic state then tunnels through the insulating alumina film into the NiAl substrate. The fluorescence depends strongly on the molecular configuration. However, for the same conformation, emission is almost identical. This is shown in Figure 15, where the light emission spectra were acquired over one of the smaller lobes of three different saddle molecules with different Ag and W tips (Figure 15A). Using the same tips, spectra of the clean NiAl surface were obtained (Figure 15B). The difference for each pair of spectra is then plotted in Figure 15C. The three curves show that the intrinsic emission from the three molecules is virtually identical and is independent of the tip. This suggests that the fluorescence peaks (Figure 15A) originate in the molecule before generation of a tip plasmon rather than direct plasmon excitation.[85,86]

There are relatively few examples of hole attachment to an occupied orbital (Figure 4b), producing a positively charged species. This requires a negative voltage on the surface, $V_S < 0$. Using this method, hydrogen atoms have been desorbed from the hydrogenated Si(100) surface.[87] The desorption of hydrogen was studied over a voltage range from -5 to -10 V and the current measured for a fixed desorption rate of 4 s^{-1} (50% desorption at a scan rate of 2 nm s^{-1}). A minimum in the desorption current corresponding to a maximum in the efficiency was observed at -7 V. For a fixed voltage, the variation of the desorption rate versus the current was fitted with a power law, I^N, where $N = 6$. The results were interpreted similarly to those of electron attachment. Here, an electron tunneling from the sample to the tip may excite a σ(Si−H) bonding orbital and transfer energy to the hydrogen atom. This process was viewed as inelastic scattering of a tunneling hole with a σ(Si−H) hole resonance (Figure 16). Calculations were used to explain the difference in the power law exponent between the electron attachment case[46] where $N = 13$ and these results with $N =$

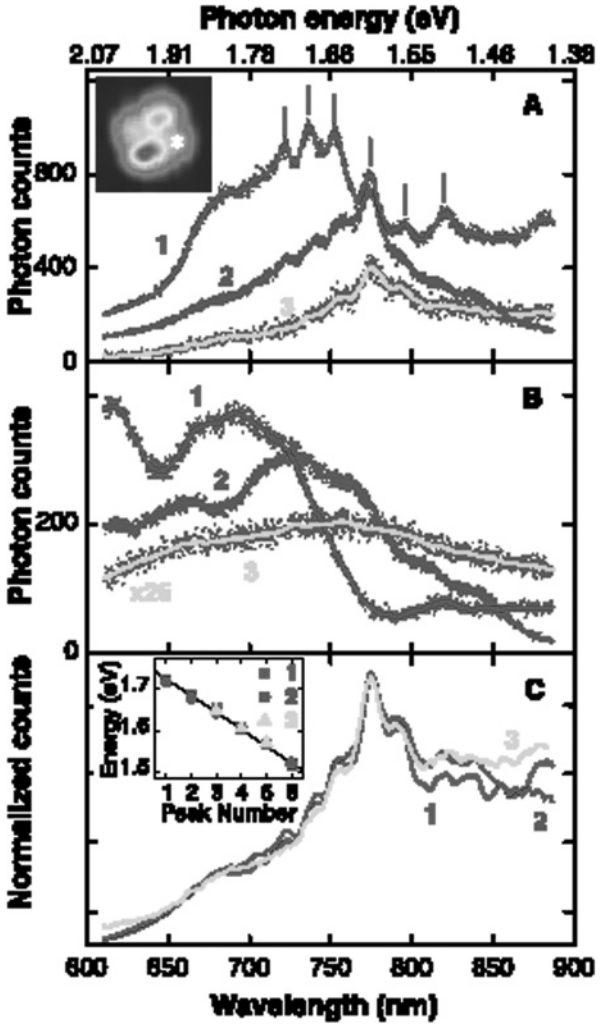

Figure 15. (A) Light emission spectra for three different experimental runs with three different tips. The spectra were acquired over one of the smaller lobes of the saddle molecules, as marked in the inset image. The raw data are plotted together with the corresponding smoothed curves (colored lines) to facilitate the identification of the peaks (red bars). Spectra 1 ($V_{bias} = 2.35$ V, $I = 0.5$ nA, exposure time 300 s) and 2 ($V_{bias} = 2.35$ V, $I = 0.6$ nA, exposure time 200 s) were taken with two different Ag tips. Spectra 1 and 2 have been offset vertically for clarity. Spectrum 3 ($V_{bias} = 2.3$ V, $I = 1$ nA, exposure time 600 s; the original data have been multiplied by 3) was obtained with a W tip. The differences in the spectra are caused by different tip plasmon properties. In particular, because of the higher amount of dielectric losses characteristic for W, the emission rate for the W tip is ~30 times lower. (B) NiAl light emission spectra measured with the same tips as in (A). The curve sequence is consistent with that of (A). The raw data are plotted together with the corresponding smoothed curves (colored lines). The spectra were acquired with the same voltages as in (A) and scaled so that the photon yields of the different tips could be directly compared (the differences in the levels of statistical noise are caused by the different acquisition times for the three spectra; the data of curve 3 have been multiplied by 25). (C) Smoothed molecular spectra from (A), divided by the corresponding smoothed NiAl spectra from (B) and normalized to the same scale. The inset shows the photon energy of each peak determined for the three spectra, as marked in (A). Reproduced with permission from *Science* (http://www.aaas.org), ref 83. Copyright 2003 American Association for the Advancement of Science.

6. The calculations indicated that the different lifetimes between the σ(Si−H) and σ^*(Si−H) orbitals modified the inelastic scattering. Furthermore, the calculations showed that the maximum desorption rate at -7 V was due to the fraction

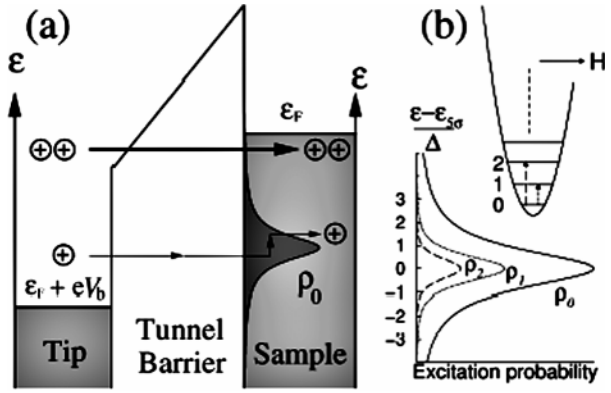

Figure 16. STM tip-induced desorption of H atoms from the hydrogenated Si(100)-2×1 surface. (a) Inelastic tunneling of a hole into an adsorbate-induced hole resonance with the density of states ρ_0. The higher barrier for tunneling into the hole resonance compared to tunneling into Fermi-level states means that only a fraction of the total tunnel current will pass through the hole resonance. (b) Schematic illustration of relative energy dependent probabilities $\rho_n(\epsilon)$ for inelastic hole tunneling with energy transfer $nh\omega_0$ to the adsorbate. Reproduced with permission from ref 87 (http://link.aps.org/abstract/PRL/v80/p2618). Copyright 1998 American Physical Society.

of inelastically scattered electrons being maximum at the onset of the field emission regime.

In fact, both elastic and inelastic tunneling of electrons (holes) from the tip can occur through the unoccupied (occupied) orbitals of the adsorbed atom or molecule. The quantum efficiency of the inelastic process (number of inelastic events relative to the total number of tunneling electrons) can vary within a very broad range, typically from 10^{-10} to 10^{-4}, depending on the studied system.[88]

3.2. Electronic Transition

Inelastic tunneling of electrons (Figure 4c) or holes (Figure 4d) can also induce an electronic transition, i.e., the transition of an electron from an occupied orbital to an unoccupied orbital, in the adsorbed atom or molecule. This process should occur at a higher surface (tip) voltage compared to the electron (hole) attachment, such that the electrons are no longer in the tunnel regime but rather in the field emission regime.

The most documented example is the $\sigma \rightarrow \sigma^*$ electronic transition of the Si−H bond producing the desorption of individual hydrogen atoms from the hydrogenated Si(100):H surface.[49,57,58] This electronic transition occurs at a surface voltage of $V_S \approx 8$ eV, which indicates that the electrons are emitted by the STM tip in the field emission regime. Indeed, the desorption yield is high (2.4×10^{-6} H atom per electron). This is related to the long vibrational lifetime of the excited state of the Si−H bond[61] on the order of 10 ns and is due to the fact that the Si−H bond can only relax via phonon coupling to the surface,[89] whereas on metals, electron−hole pair (EHP) formation is more favorable and therefore more rapid. It should be noted that the vibrational relaxation time due to EHP excitation is in the picosecond range while that due to phonon coupling is in the nanosecond range.[90]

Another example of STM manipulation leading to a modification on the atomic scale via an induced electronic transition is the desorption of silicon adatoms from the Si-(111)-7×7 surface.[91] Here, by applying either a positive or a negative sample bias, both electrons and holes could induce desorption (Figure 17). A threshold was observed around

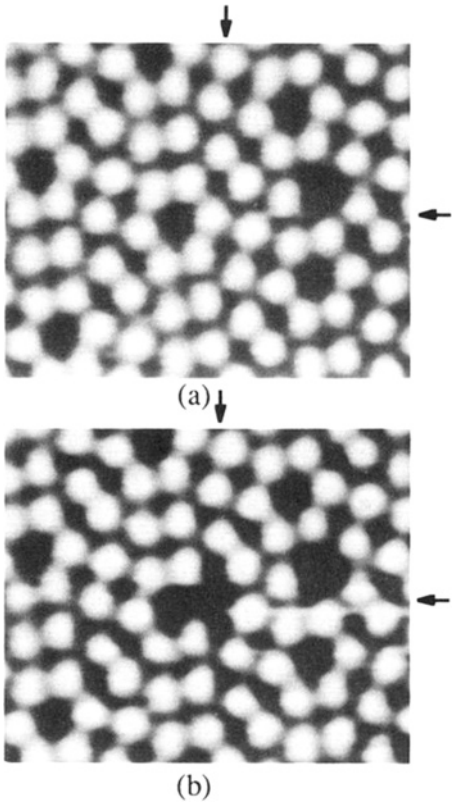

Figure 17. Single silicon vacancy creation on the Si(111)-7×7 surface. The STM tip was positioned at the point indicated by the arrow in the first image. After a −4 V pulse to the sample, a single vacancy appears at that point. Both images were taken at a sample bias of +2 V and 0.6 nA. Reproduced with permission from ref 91 (http://link.aps.org/abstract/PRL/v70/p2040). Copyright 1993 American Physical Society.

+4 V and at a slightly lower negative voltage since at −4 V a few single-atom events were observed. At ±6 V, about 10 vacancies were created during a single 10 ms pulse. These vacancies cover roughly 100 nm^2, which is consistent with the field emission regime. There is no explicit mention of the nature of the induced electronic excitation process.

The $\sigma \rightarrow \sigma^*$ electronic transition producing the desorption of hydrogen atoms on the hydrogenated Si(100):H surface has also been investigated by laser excitation. In their experiment, Vondrak and Zhu investigated hydrogen desorption using direct optical excitation at 157 nm.[92,93] The photon energy of 7.9 eV corresponds to the direct $\sigma-\sigma^*$ transition of the Si−H bond. From the detection of atomic hydrogen by time-of-flight (TOF) measurements using both the p-polarization and the s-polarization, they were able to deduce that the transition dipole moment was at 18° to the surface normal, which agrees very well with the calculated Si−H bond angle.[94] This led them to conclude that hydrogen desorbs via a one-photon direct optical excitation of the dipole. However, the lack of sensitivity in the TOF detection of the hydrogen ions desorbed by the laser obliged them to use a high irradiation dose of 300 J·cm^{-2}. In this regime, other indirect processes could occur which might not have been detectable.

Laser excitation producing the desorption of hydrogen from the hydrogenated Si(100)-2×1:H surface has been studied further on the atomic scale by combining in one experiment a laser and the STM.[95,96] In these studies, a laser at 157 nm was used to induce hydrogen desorption with low irradiation doses from 1 to 23 J·cm^{-2} to avoid thermal

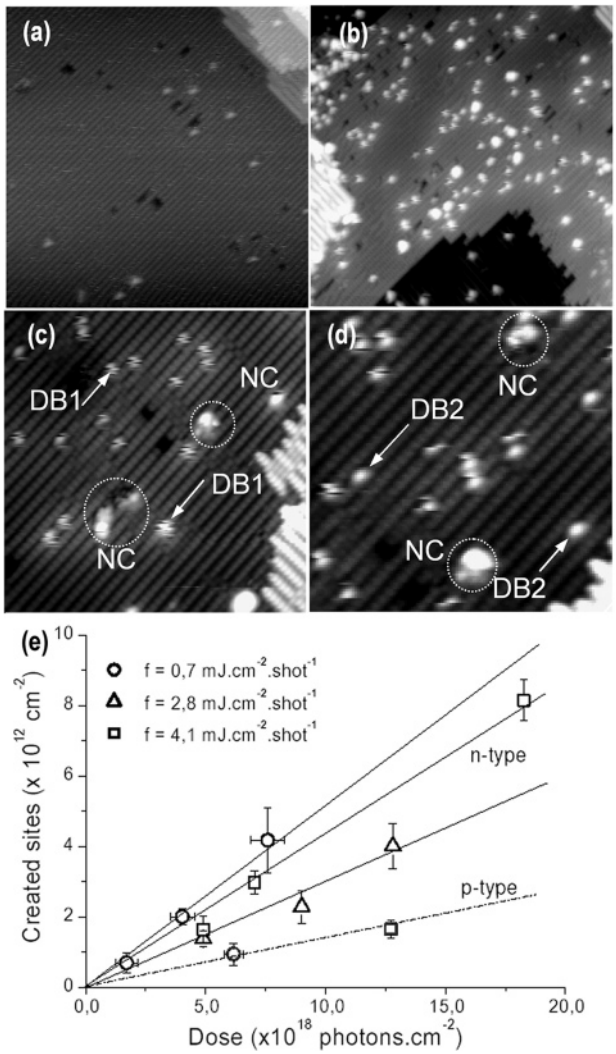

Figure 18. Laser desorption of hydrogen from a Si(100)-2×1:H surface. STM topographies from n-type samples acquired at $V_S = -2.5$ V and $I_t = 150$ pA. Key: (a) 40 × 40 nm^2, hydrogenated surface before irradiation; (b) 40 × 40 nm^2, surface after irradiation at 157 nm with a dose of 6 J·cm^{-2} at 2.8 mJ·cm^{-2}·shot^{-1}; (c) 16 × 16 nm^2, illustration of hopping dangling bonds observed after irradiation noted as DB1; (d) 16 × 16 nm^2, illustration of fixed sites observed after irradiation noted as DB2 (NC = noncounted site); (e) variation of the number of isolated dangling bonds by created VUV light (157 nm) on the hydrogenated Si(100) surface as a function of the irradiation dose for three different fluences and for two types of dopant. Reproduced with permission from ref 95 (http://link.aps.org/abstract/PRB/v72/p233304). Copyright 2005 American Physical Society.

heating. This was done using three different energy pulse densities of 0.7, 2.8, and 4.1 mJ·cm^{-2}·shot^{-1} on both n-type and p-type samples. Through a statistical analysis of the STM images obtained after irradiation, the number of new individual silicon dangling bonds produced was counted (Figure 18). It was found that the desorption yield was 3 times higher for the n-doped samples than the p-type samples. In addition, on the p-type surfaces, local modifications of the surface were observed in the STM images. These were ascribed to inhomogeneous laser-induced atomic-scale charging. This could be explained by the creation of additional B−H complexes in the subsurface region,[97] which deactivates the boron dopant in the case of p-type samples.[98] This positive charging of the surface explains the reduced photodesorption cross-section of p-type samples. These results suggest that considering only the direct photodesorption mechanism is an oversimplified view of vacuum ultraviolet (VUV) laser photodesorption. Complex surface and subsurface processes such as local charging should be taken into account if we are to fully understand VUV photochemistry on the Si(100):H surface.

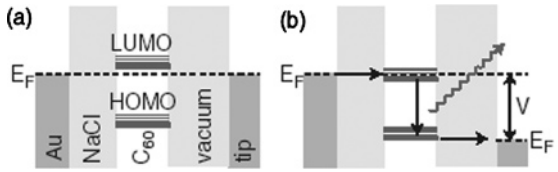

Figure 19. STM-induced photon emission from C_{60} molecules adsorbed on a NaCl layer on the Au(111) surface. Schematic energy diagram of the double-barrier tunneling junction at (a) zero-bias voltage and (b) applied negative voltage, corresponding to the conditions for luminescence. Reproduced with permission from ref 99 (http://link.aps.org/abstract/PRL/v95/p196102). Copyright 2005 American Physical Society.

3.3. Electron–Hole Pair Attachment

Another type of electronic excitation of a molecule is the simultaneous attachment of an electron to an unoccupied π^* orbital and a hole to an occupied π orbital. Such an electronic scheme can only occur if the molecule interacts weakly with both the STM tip and the surface. In such a case, the orbital energies of the molecule can be shifted by the electric field between the tip and the surface as shown in Figure 4e,f.

The photon emission from C_{60} molecules induced by the STM tip presents an interesting case.[99] Here, NaCl was deposited on a Au(111) substrate, creating an insulating layer between one and three monolayers thick. C_{60} molecules were then deposited, forming truncated triangular islands in which the C_{60} molecules are arranged in hexagonal arrays. Light emission from C_{60} is observed only for biases higher than a threshold voltage of $V = -2.3$ V. The emission onset was at 680 nm, and its position was independent of the voltage. The observation of the luminescence is explained by the relative positions of the molecular levels to those of the tip and the surface. Below −2.3 V, the highest occupied molecular orbital (HOMO) is above the Fermi level (E_F) of the tip. Electrons are extracted from the HOMO and tunnel to the tip. At the same time, the lowest unoccupied molecular orbital (LUMO), which is below the Fermi level of the sample, is populated by the electrons tunneling from the substrate (Figure 19). Photon emission occurs by the radiative decay of these electrons into the partially empty HOMO (by hot electron or hole injection). No photon emission was observed for positive bias voltages (tip to surface) below +4.5 V. This may be due to the asymmetry of the HOMO−LUMO gap with respect to E_F [100] and/or to the different properties of the two tunneling barriers (vacuum and NaCl).[101] Further analysis of the spectra, after correction for the quantum efficiency of the detection system, showed the presence of both fluorescence and phosphorescence (Figure 20). The spectra were compared with earlier laser-induced high-resolution photoluminescence data[102,103] and quantum chemical calculations.[102,104] Two forms of spectra were observed, one with a peak at 750 nm and an onset at around 680 nm and another with two peaks at 720 and 800 nm. The first spectrum was interpreted as a pure electronic $S_0 \leftarrow S_1$ transition with an internal structure showing a clear vibronic progression. Normally, electric dipole transitions to the ground state are symmetry forbidden, but they can occur through the Herzberg−Teller and Jahn−Teller electron-

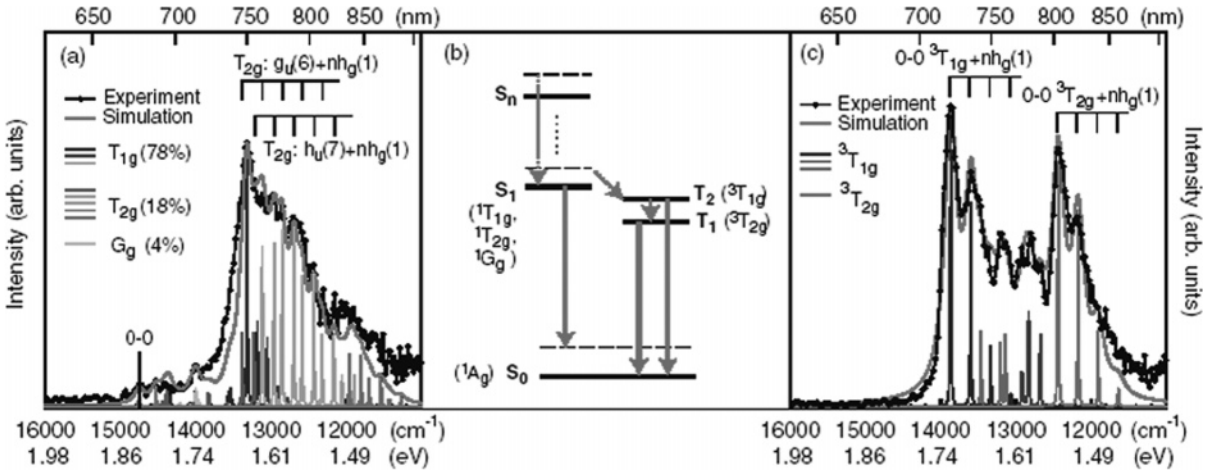

Figure 20. (a) STM-induced light emission spectrum assigned to C_{60} fluorescence ($V = -3$ V, $I = 1$ nA) and calculated spectrum. (b) Schematic diagram of the lowest singlet (S_i) and triplet (T_i) states: horizontal solid lines, pure electronic levels; horizontal dashed lines, vibrational levels. Solid arrows represent electronic transitions; dashed arrows represent radiationless mechanisms of relaxation (internal conversion, intersystem crossing, vibrational relaxation). (c) STM-induced light emission spectrum assigned to C_{60} phosphorescence ($V = -3$ V, $I = 1$ nA) and calculated spectrum. For both simulations, experimentally determined frequencies for the vibronically induced $S_0 \leftarrow S_1$ (T_{1g}, T_{2g}, G_g) and $S_0 \leftarrow T_1$ ($^3T_{2g}$), T_2 ($^3T_{1g}$) transitions are used. Each component has a Lorentzian line shape, broadened by 150 cm^{-1} (a) and 200 cm^{-1} (c) to obtain the calculated spectra. Reproduced with permission from ref 99 (http://link.aps.org/abstract/PRL/v95/p196102). Copyright 2005 American Physical Society.

vibration coupling mechanisms of intensity borrowing.[104] The second type of spectrum was explained by the phosphorescence of the C_{60}. This could be fitted by a triplet−singlet $S_0 \leftarrow T_1$ transition characterized by an intense 0−0 origin at 800 nm and a vibronic progression of a Jahn−Teller active mode. The higher energy peak (at 720 nm) was assigned to the next highest triplet state, $S_0 \leftarrow T_2$.

3.4. Competing Processes: Photon Emission

It should be emphasized that inelastic tunneling of electrons (IET) or holes can also induce the emission of photons in the tunnel junction.[105−109] This involves inelastic tunneling from the tip electronic states into the lower lying states of the sample with the simultaneous release of the excess energy in the form of a photon. Such an emission of photons is in competition with the electronic excitation process described in sections 3.1, 3.2, and 3.3.

This competing photon emission process has been observed on the partially dehydrogenated Si(100) surface.[108,109] Thirstrup and coauthors have used the STM to desorb hydrogen atoms and to study the light emission induced from atomic-scale patterns of silicon dangling bonds on the hydrogenated silicon surface.[110] They obtained spatial maps and spectroscopy of silicon dangling bond patterns on the 3 × 1 surface (Figure 21). By observing that the wavelength of the emitted photons changed as a function of the bias voltage on the tip, they proposed that the light emission involved optical transitions between a tip state and localized surface states. They found that the spatial maps were comparable to the STM images and hence deduced that the photons are emitted from a quasi-point source corresponding to the dangling bonds. In a subsequent study on the deuterated 2 × 1 surface the switching of individual silicon dangling bonds could be observed.[111]

It should be noted that the limited spatial resolution of optical excitations using lasers or other photon sources (on the order of the wavelength) is compatible with a single-molecule operation only by diluting the number of molecules adsorbed on a surface[112] or by working in the high-resolution spectroscopic regime of molecules trapped in matrixes at low temperature.[113] Again, the environment around each molecule can have a significant impact of the behavior of the molecule. In addition, optical irradiation will not only excite the molecules directly but also create secondary electrons in the substrate which cause indirect excitation of the molecules. Thus, interpretation of these experiments becomes more complicated.

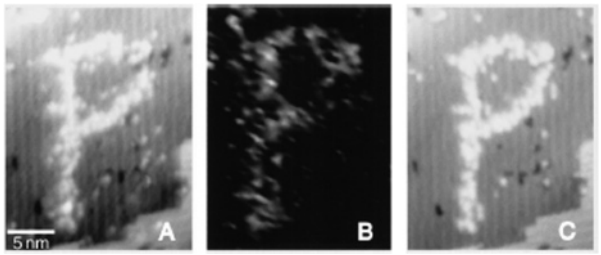

Figure 21. (A) STM topographic filled state image of exposed dangling bonds forming the letter P on a Si(001)-3×1:H surface ($V_b = -2$ V, $I_t = 0.2$ nA, scan speed 1400 nm/s). (B) Photon map recorded at the same area as in (A) using $V_b = -3$ V, $I_t = 8$ nA, and $y_S = 9$ nm/s. (C) STM topographic image recorded after the photon map and with the same scanning conditions as in (A). The size of the letter P is 17 nm. Reproduced with permission from ref 110 (http://link.aps.org/abstract/PRL/v82/p1241). Copyright 1999 American Physical Society.

3.5. Competing Processes: Electric Field Effects

In manipulation experiments where a voltage pulse is applied to excite an adsorbed atom of a molecule, the flow of current implies the presence of an electric field between the tip and the surface. In addition to the process of electronic excitation, the electric field can be used to manipulate atoms or molecules by inducing a local dipole in the adsorbed species. Another effect of the electric field is to reduce the barrier height between the tip and the surface, increasing the probability of inducing a reaction.[114] The major difficulty is to distinguish between these different processes as they are in competition.

Several experiments have used the electric field to manipulate atoms. Small clusters of silicon atoms were

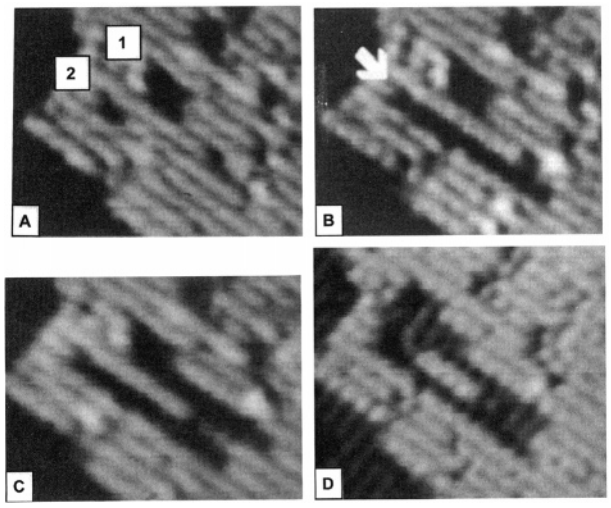

Figure 22. Fabrication of an island one dimer wide on Si(001). (A) Two pits fabricated using threshold voltages at $s = 1.5$ Å (pit 1) and $s = 1.1 \pm 0.3$ Å (pit 2). (B) Trench one dimer wide and nineteen dimers (77 Å) long that was fabricated by repeatedly removing atoms from an individual dimer row, starting at the lower right end of pit 2. (C) Situation after formation of another single-dimer-wide trench starting from the bottom row of pit 1. (D) Fabricated island that is one dimer wide and five dimers long, isolated by a moat one atomic layer deep. All images are 130 × 100 Å^2. Reproduced with permission from *Science* (http://www.aaas.org), ref 116. Copyright 1994 American Association for the Advancement of Science.

removed from the Si(111)-7×7 surface[115] by moving the tip toward the surface, thus increasing the electric field. The tip displacement versus current curves showed the presence of abrupt steps, indicating the formation of a mound of atoms under the tip followed by an atomic bridge which broke as the tip retracted. The minimum field necessary to induce desorption was estimated to be greater than 1 V/Å. This method was used to etch small atomic sized pits on the Si-(100)-2×1 surface.[116] In this experiment, the electric field was estimated to be around 2 V/Å. Figure 22 shows the controlled desorption of silicon dimers to form different structures on the surface.

3.6. Competing Processes: Direct STM Tip–Surface Interaction

The dynamics of single atoms or molecules can be induced by the STM tip even though the surface voltage is zero; i.e., there is no tunnel current, and the electric field is negligible or nonexistent. This is achieved when the tip is brought close to the surface, such that the direct STM tip−surface interaction is strong enough to weaken the interaction between the manipulated atom or molecule and the surface. Not only weak van der Waals bonds but also strong chemical bonds can be broken in this way.

This effect has been demonstrated by the vertical manipulation of individual germanium atoms from a Ge(111)-c(2×8) surface at room temperature.[117] Indeed, when the tip apex−surface distance is greatly reduced, the potential barrier to transfer a chemically bound Ge atom from the surface to the tip vanishes. Using this method, individual Ge atoms could be picked up with the STM tip in a very controlled manner (Figure 23) without any tunneling electron or electric field effect. Surprisingly, the duration of the excitation mechanism was found to be very long (10 ms) compared to intrinsic relaxation times.[117] A possible explanation for this

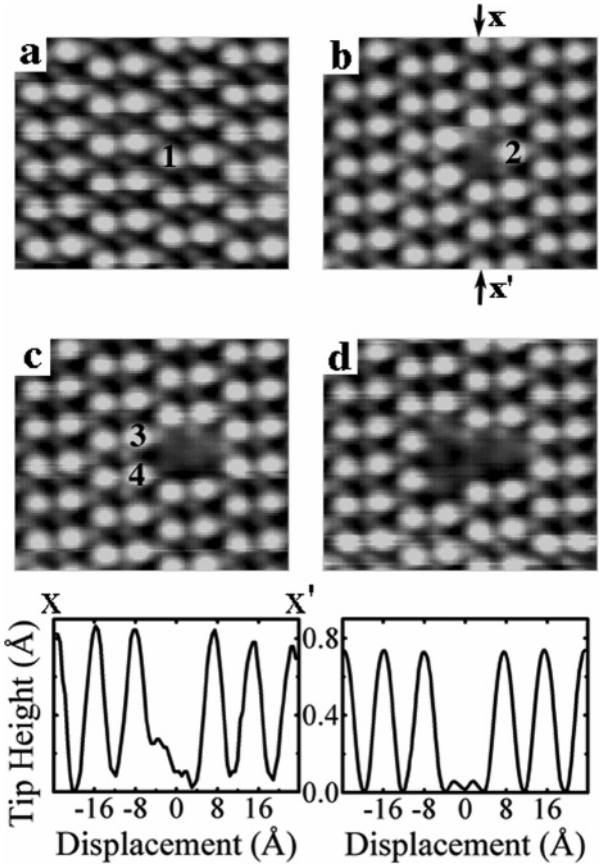

Figure 23. Sequence of STM images of the Ge(111)-c(2×8) surface [from (a) to (d)] during which atoms were extracted (area 53 × 47 Å^2, sample bias +1 V, tunnel current 1 nA). The selected atoms are indicated by numbers 1−4. A line profile *xx′* through (b) is shown at the lower left and a corresponding calculated line profile, for $I = 1$ nA at the bottom of the conduction band, at the lower right. Reproduced with permission from ref 117 (http://link.aps.org/abstract/PRL/v80/p3085). Copyright 1998 American Physical Society.

long reaction time is that a large potential basin is created by the constraint of the tip apex, opening the way for the targeted Ge atom to diffuse around the end atom on the tip apex in a complex and long trajectory.

At larger tip−sample separations, the field-induced desorption mechanism could be brought into play whereby single Ge adatoms could be removed using positive sample biases.[117] By increasing the applied voltage during the pulse, the probability of desorbing a Ge atom from the surface increased. This result agrees with those of the original STM manipulation studies on the Ge surface.[31]

4. Electronic Control of Molecular Dynamics

We will review here a number of examples of molecular dynamics induced by electronic excitation which have been studied with the STM. In most of these studies, irreversible dynamical processes have been induced mainly in the form of molecular dissociation.[34,118] It is important to note that the concept of control has greatly changed over time. Initially, control implied triggering the molecular dynamics by applying a pulsed voltage between the STM tip and the surface. The control parameters were the surface voltage V_S, the tunnel current I_S, and the duration of the excitation. The dynamics of a single molecule could be monitored in several ways. The most commonly used is to image the molecule

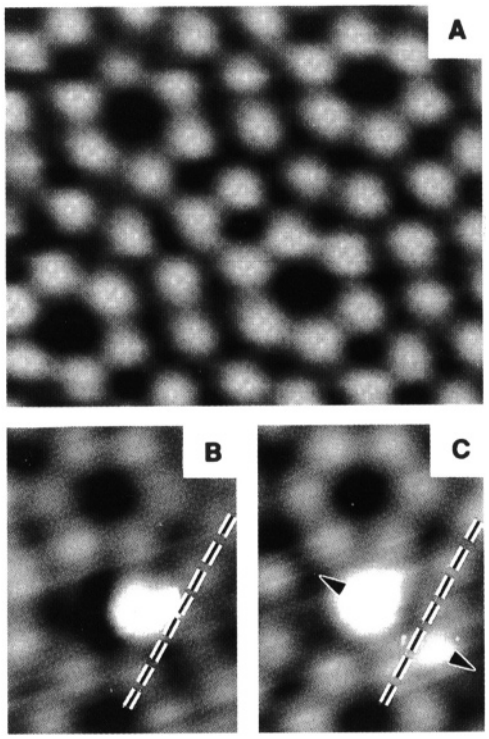

Figure 24. (A) STM image of the clean Si(111)-7×7 surface with the sample biased to +2 V. (B) Isolated $B_{10}H_{14}$ molecule (large white spot) adsorbed next to a dark defect. (C) Result of electron bombardment at a bias voltage of +8 V. A large molecular species is now located over the original defect, and an additional fragment (small white spot) is seen to the lower right. The lateral distance between the large dark "corner holes" of the Si surface is 27 Å, and the color scale indicates a vertical range of 1 Å from black to white. Reproduced with permission from *Science* (http://www.aaas.org), ref 34. Copyright 1992 American Association for the Advancement of Science.

with the STM before and after the electronic excitation and to examine the induced changes. However, more detailed information on the molecular dynamics can be obtained by recording the tunnel current during the electronic excitation.[31,35,36,51,52,80,115] Any change of the molecular configuration can thus be followed in real time. Of course, the time resolution is limited by the band-pass of the tunnel current detection. With the advent of more complex molecular dynamics studies, control is no longer just the ability to trigger the molecular dynamics in a precise and reproducible manner. The demonstration of electronic control requires the presence of at least two different molecular dynamical channels and the ability to activate each of them selectively.

4.1. Single-Molecule Chemistry on Semiconductor Surfaces and Electronic Excitation

The first molecular dynamics induced by electronic excitation with the STM was the dissociation of a decaborane molecule ($B_{10}H_{14}$) adsorbed on a Si(111)-7×7 surface.[34] This molecule was adsorbed on the Si(111)-7×7 surface and could be seen as a bright protrusion 2 Å high, preferentially adsorbed near defects (Figure 24). The dissociation was induced by applying a surface voltage above a threshold of +4 V. Electronic excitation was considered to be the cause of the dissociation because the estimated electric field on the order of 0.7 V/Å was thought to be too low to play a dominant role.

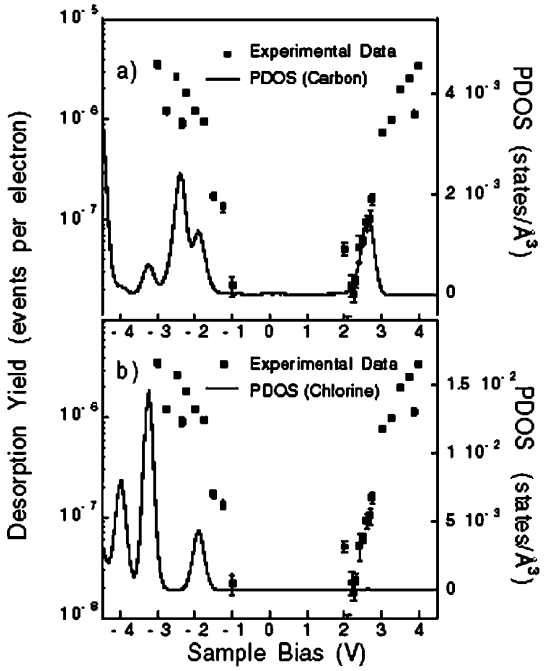

Figure 25. Experimental desorption yield per electron of C_6H_5Cl molecules from the Si(111)-7×7 surface as a function of the sample bias voltage in the STM (black squares), compared with the (solid lines) calculated partial density of p states at (a) the carbon atom in the ring and (b) the chlorine atom (for details see the text). Reproduced with permission from ref 120 (http://link.aps.org/abstract/PRL/v91/p118301). Copyright 2003 American Physical Society.

Electron-induced dissociation or desorption has also been performed on halobenzenes. There have been several experiments on chlorobenzene (PhCl) adsorbed on the Si(111)-7×7 surface. The first study[119] had shown that PhCl molecules adsorbed on the Si(111)-7×7 surface could be dissociated using voltage pulses of +4 V for 10 ms. It was found that the chlorine atoms were attached to silicon atoms on neighboring sites after dissociation. Thus, the process of electron attachment followed by bond cleavage of the anion and formation of a Si−Cl species was interpreted as being a concerted process. More recently,[120] it was found that the dominant channel of STM manipulation depended on the condition of the tip. Two different tips were found to exist; if the molecule was observed as a depression at sample bias voltages of both +1 and +2 V, then dissociation could be induced. However, if the molecule was seen as a protrusion at +2 V, then the tip induced desorption. In addition, desorption was found to occur at both polarities,[120] whereas dissociation occurs only at positive sample voltages.[118]

Desorption experiments[120] as a function of both voltage and current showed that the desorption yield was constant for different tip−sample separations. Two clear thresholds were observed at −1.5 and +2.5 V (Figure 25), and the desorption rate showed a linear dependence on the current. This indicated that vibrational heating, electric field, and mechanical effects were not dominant. The desorption mechanism was interpreted as being driven by the population of the negative (or positive) ion resonance state[44] of the chemisorbed chlorobenzene molecule. Comparison with the density of states calculated using density functional theory suggested that these resonance states were associated with the π orbitals of the molecular benzene ring.

The dissociation process has been studied recently in more detail by Sloan and Palmer.[118] Dissociation was induced by

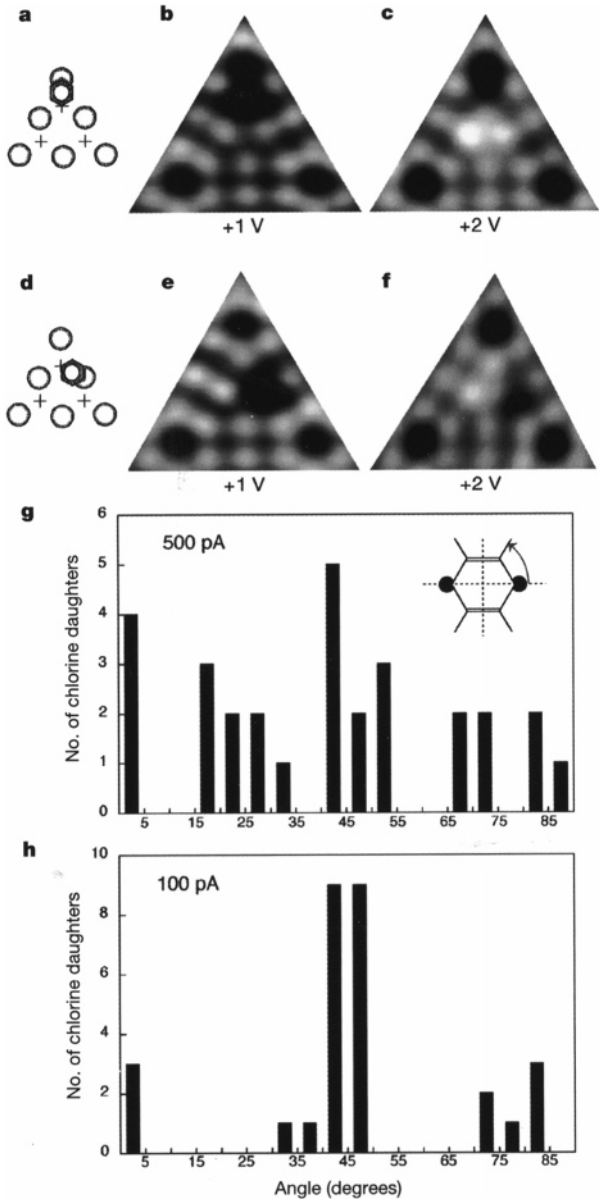

Figure 26. Angle-resolved dissociation of C_6H_5Cl molecules on the Si(111)-7×7 surface. (a−f) STM images and schematic diagrams (circles represent adatoms, crosses represent rest atoms, and hexagons represent chlorobenzene molecules), showing the imaging characteristics of a single adsorbed molecule as a function of the sample bias (50 pA, bias voltages as marked): (a−c) chlorobenzene bonded to a corner adatom; (d−f) chlorobenzene bonded to a center adatom. Note the bright feature that appears over the bonding rest atom in the case of a corner-bonded chlorobenzene molecule. This signature allows us to identify which of the two candidate rest atoms is the bonding rest atom when a chlorobenzene molecule is bonded to a center adatom. (g) Inset, diagram of the chlorobenzene adsorbate (filled circles represent the bonding silicon atoms), showing the planes of symmetry (dashed lines) and angular coordinate system (arrow). (g, h) The angular distribution (5° bins) of daughter chlorine atoms, relative to the adatom/rest atom axis of each corresponding parent chlorobenzene molecule (inset), is generated by tunneling currents of 500 pA (g) and 100 pA (h). Reproduced with permission from *Nature* (http://www.nature.com), ref 118. Copyright 2005 Nature Publishing Group.

scanning the surface at +4 V, and the current dependence suggests a two-electron process. Until now most examples of multiple-electron processes involve the same ground and excited states. In this experiment, coupling between two different orbitals is required for the chlorine atom to be

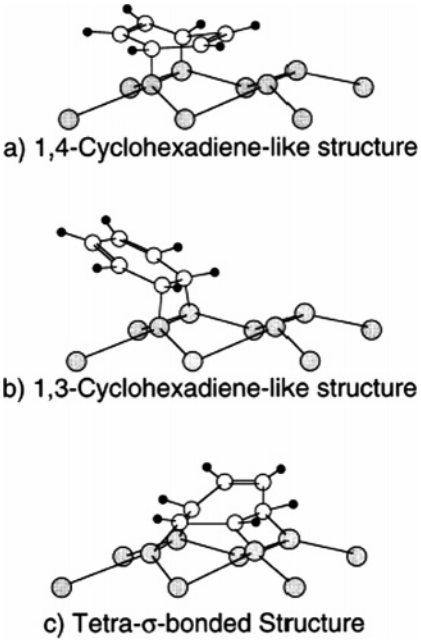

Figure 27. Geometrical representation of benzene chemisorbed on Si(100)-2×1: (a) 1,4-cyclohexadiene-like structure; (b) 1,3-cyclohexadiene-like structure; (c) tetra-σ-bonded structure suggested by Lopinski et al.[129] Reproduced with permission from ref 131. Copyright 1998 Elsevier.

ejected. Coupling between the π^* orbital of the molecule and the σ^* orbital of the C−Cl bond occurs via vibrational excitation of the out-of-plane C−Cl bending mode.[121] This $\pi^*-\sigma^*$ coupling is "symmetry forbidden". The first electron populates the antibonding π^* orbitals of the phenyl ring initiating the process.[122] However, dissociation requires a second electron to attach to the σ^* orbital of the C−Cl bond, creating a negative chlorine ion, that is, dissociative electron attachment (DEA).[123,124] The average time interval between two tunnel electrons depends on the current, so if the arrival of the second electron occurs while the chlorobenzene is in a more vibrationally excited state, then coupling will be more efficient to the C−Cl bond. This is confirmed by the radial and the angular distributions (Figure 26) determined from the chlorine position relative to the initial configuration for each molecule dissociated.[120,125,126]

Desorption of benzene molecules from the Si(100)-2×1 surface has also been studied in detail. At room temperature, STM images of benzene adsorbed on the Si(100)-2×1 surface shows the presence of two different bonding configurations.[127−129] This has been confirmed by angle-resolved ultraviolet photoemission spectra[130] and NEXAFS studies.[131] These experimental studies were combined with various structure calculations,[128,129] suggesting the presence of a metastable site where the benzene is on top of a single Si dimer and a more stable site where the benzene bridges two dimers (Figure 27). At room temperature, benzene adsorption occurs initially in the metastable site followed by thermally driven conversion to the more stable site with an estimated barrier of 0.95 eV. Furthermore, in this study,[128,129] the STM tip could induce conversion from the stable site back to the metastable site (Figure 28). By scanning at −3 V and 40 pA, while some molecules are desorbed, 75% of the remaining molecules are converted back to the on-top single-dimer site. The barriers to desorption and reconversion were estimated to be 0.77 and 0.75 eV, respectively. In a subsequent study,[132,133] STM manipula-

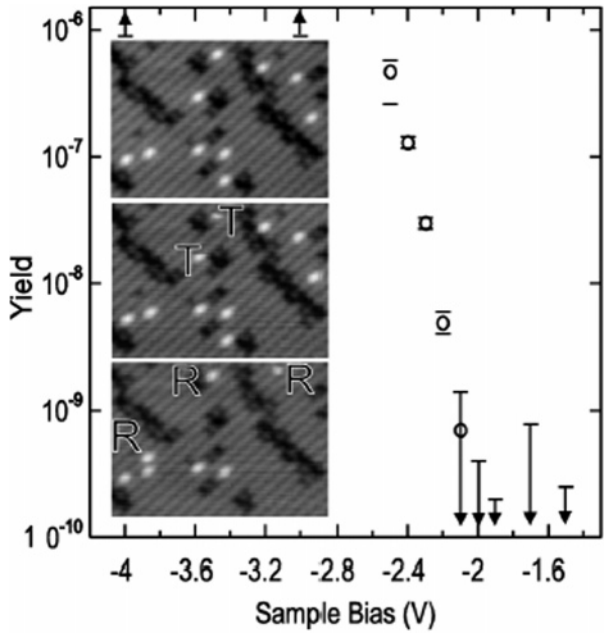

Figure 28. Desorption yield for benzene on Si(100) as a function of the sample bias at 22 K. The inset shows successive STM images (42 pA, −2.3 V, 150 × 110 Å^2, 300 nm/s). Examples of molecules desorbing during the scan are marked "T", while readsorbed molecules are labeled "R". Reproduced with permission from ref 133 (http://link.aps.org/abstract/PRL/v85/p5372). Copyright 2000 American Physical Society.

tion of the on-top single-dimer site was carried out by stabilizing the benzene molecules at low temperature (22 K). Desorption of the benzene molecules could be induced by applying a negative sample bias to the tip. A threshold was observed at −2.0 V with a rapid rise in the desorption probability peaking at −2.5 V with a yield of 10^{-6} event per electron (Figure 28). An electronic excitation of the $\pi-\pi^*$ transition was not considered to be involved since this $\pi-\pi^*$ transition was estimated to be about 4.5 eV.[130] However, in the same photoemission study, a C−C π bonding state was identified at 2.3 eV below the Fermi level.[131] The bond-breaking mechanism in the desorption of benzene at low temperature was believed to involve resonant excitation of this surface state. The positive ion resonance formed by the electron leaving the molecule relaxes when an electron hops from the substrate to the molecule. Computation of the desorption dynamics suggested this is indeed the case.[133] The calculation indicated that excitation of the π bonding state transfers energy into the ring-bending mode and that this vibrational energy couples efficiently with the σ Si−C bond, leading to desorption. This is similar to the desorption[120] and dissociation[118] of chlorobenzene.

Polyaromatic molecules are of interest for several reasons. First, it may be possible to induce changes in the conductivity of the π system of the molecule through STM manipulation. This may cause the molecule to change conformation. Second, it may also be possible to excite one part of the molecule and induce a modification in another part of the molecule. Several STM studies have been carried out recently on such molecules. A recent study[134] has looked at the adsorption and manipulation of a 1,4″-*p*-triphenyldimethylacetone (called Trima for short). This molecule adsorbs on the Si(100)-2×1 surface at room temperature with its long axis parallel and on top of the silicon dimer row. Individual molecules were manipulated by injecting electrons into the central benzene ring with the STM tip. Different parts of

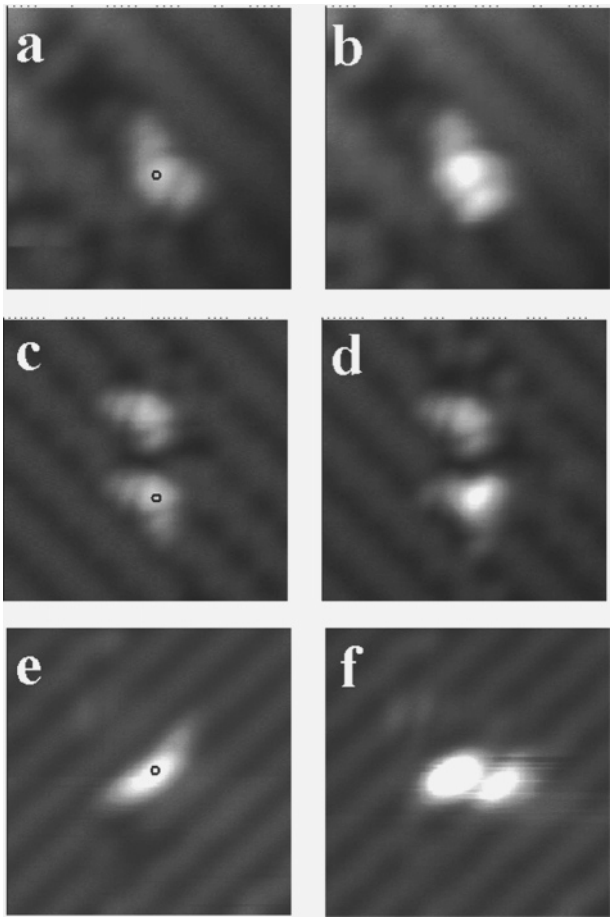

Figure 29. STM manipulation of the Trima molecule on the Si(100)-2×1 surface. Three pairs of STM images show different molecules before manipulation, (a), (c), and (e), and after manipulation, (b), (d), and (f). In each case the electrons were injected by the STM tip into the central bright part of the molecule. For a voltage pulse at a sample bias of 4.0 V (a), the end of the molecule is modified (b). For a voltage pulse of 4.5 eV (c), the center of the molecule is modified (d). For a voltage pulse of 5.0 eV (e), the molecule is dissociated (f). Note that, in images e and f, the poorer resolution is due to the tip. Reproduced with permission from ref 134. Copyright 2005 American Institute of Physics.

the Trima molecule could be selectively modified by choosing the appropriate applied bias (Figure 29). With 4.0 eV electrons, the end of the molecule changed, with 4.5 eV electrons the middle of the molecule was modified, and with 5.0 eV electrons, dissociation of the molecule was observed. Parallel photoemission studies provided important supplementary information. NEXAFS spectra showed that the C=O bond in the ketone groups reacted with the silicon surface to form C−O−Si bonds, and valance-band photoemission spectra indicated that the benzene rings had only a very weak interaction with the surface. This suggests that the Trima molecule is chemisorbed on the surface through the ketone groups. Furthermore, these studies suggested a $\pi-\pi^*$ transition at 4.5 eV. This corresponded well with the threshold of 4 eV observed in the STM manipulation experiments, indicating a direct electronic excitation of the $\pi-\pi^*$ transition.

Another example of the manipulation of a polyaromatic molecule is that of biphenyl on Si(100)-2×1.[135,136] At room temperature, the molecule was observed to adsorb in one of two configurations. In the minority site, the molecule was fixed on the surface with the long axis at 30° to the Si dimer row (Figure 30). However, the majority site appeared to be

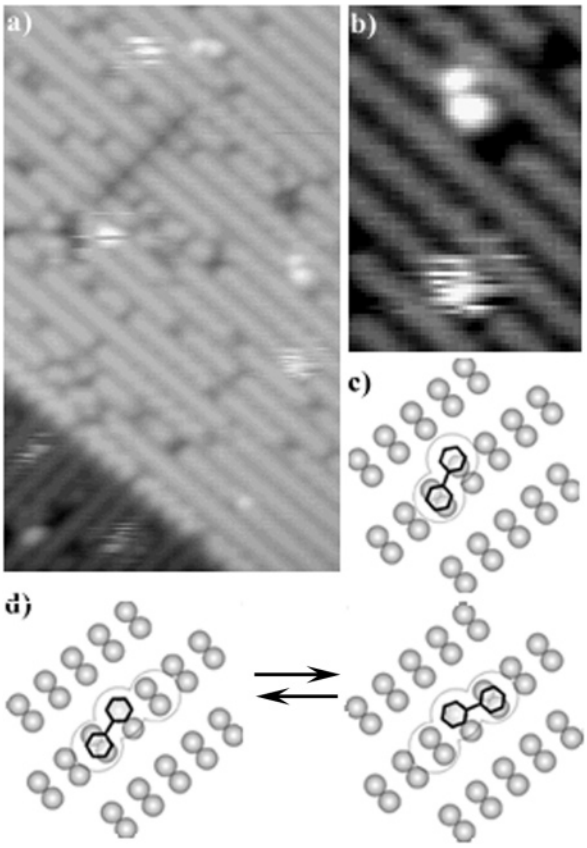

Figure 30. Biphenyl molecules adsorbed on the Si(100)-2×1 surface. An STM image recorded at constant tunnel mode at 0.5 nA using a sample−tip voltage of −1.5 V (the bias refers to the sample) at room temperature of the Si(100)-2×1 surface showing (a) the biphenyl molecules adsorbed on the 12 × 20 nm^2 area of the surface. There are two fixed molecules and five unstable molecules (the striped ones). (b) is the zoom (4 × 6 nm^2) on a pair of molecules, one fixed and one unstable. (c) shows the proposed adsorption site for the fixed molecule, and (d) shows the proposed rotation of the unstable molecule about its fixed axis. Reproduced with permission from ref 136. Copyright 2005 Elsevier.

moving as the STM tip passed over the molecule. In this study,[135] STM images obtained at 35 K (after deposition at room temperature) showed biphenyl molecules fixed to the surface but with the long axis at 20° or less to the dimer row. This suggested that the unstable molecule at room temperature was pivoting about one ring between two equivalent metastable configurations. More detailed manipulation experiments[136] showed that it was possible to transform the bistable molecule into the fixed molecule by injecting electrons. The transformation efficiency was measured as a function of the applied bias, tunnel current, and duration of the pulse (Figure 31). The efficiency increased with increasing voltage between 2 and 4.5 V and was constant (95%) from 5 to 10 V. Each data point is an average obtained from manipulating between 10 and 20 individual molecules. For each voltage, the efficiency also showed an increase before flattening out with increasing current. To distinguish between an electronic excitation and the electric field, the duration of the pulse was varied for the same voltage and current. It was found that the efficiency depends on the duration of the voltage pulse, which favors an electronic excitation. This was confirmed by calculations of the electric field using Feenstra's method.[40,42,43] It was surprising to find that the estimated field between the tip and the sample fell in the range 2.3−3.3 V/Å. This is larger than the estimated field

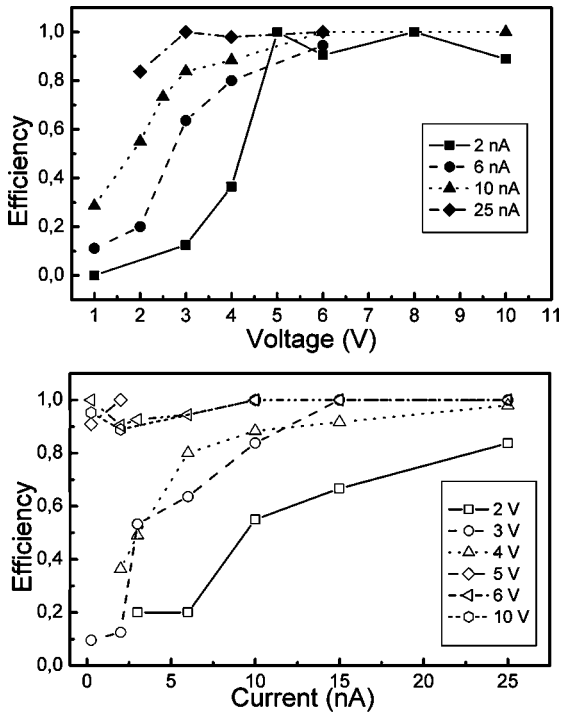

Figure 31. STM manipulation of biphenyl molecules on the Si-(100)-2×1 surface. Two graphs showing the measured efficiency of the manipulation pulses under constant-current conditions on unstable biphenyl molecules as a function of the applied voltage for different fixed tunneling currents (top) and as a function of the tunneling current for different fixed applied voltages (bottom). Reproduced with permission from ref 136. Copyright 2005 Elsevier.

applied in earlier experiments[115,116] where the electric field was the dominant mechanism and yet here appears to play only a minor role.

4.2. Single-Molecule Chemistry on Metallic Surfaces and Vibrational Spectroscopy

In 2000, Hla et al. pioneered a new field of single-molecule chemistry where a sequence of different STM manipulations was combined to synthesize a single molecule on a metal surface. This example of bond-breaking and bond-making using electronic control over a molecule is the dissociation of two iodobenzene molecules on a copper surface with the STM tip, followed by a recombination of the two phenyl groups into biphenyl.[137] This is in essence the Ullmann reaction where biphenyl is formed by heating iodobenzene with a copper catalyst.[138] In the STM experiment,[137] iodobenzene molecules were adsorbed on the Cu(111) surface at 20 K. The molecules adsorb preferentially at step edges. Tip-induced dissociation was performed by injecting 1.5 eV electrons into the iodobenzene molecules. The result was the separation of the molecule into two fragments. This was then repeated on another molecule. Lateral manipulation techniques[139−141] were then used to displace the iodine atoms away and to bring the two phenyl groups together (Figure 32). A 0.5 V pulse for 10 s was applied to the two phenyl fragments simultaneously. Afterward, the formation of a C−C bond between the two fragments could be confirmed by displacing laterally the biphenyl as a single entity.

The main difficulty when producing bond-breaking and bond-making at the level of a single molecule is to identify the products of these reactions. Wilson Ho's group has

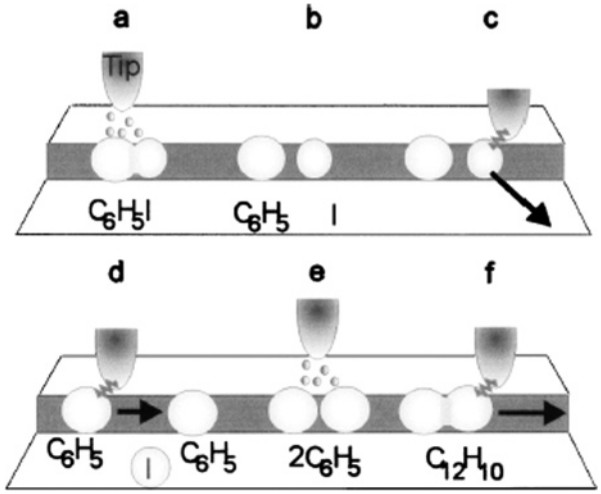

Figure 32. Schematic illustration of the STM tip-induced synthesis steps of a biphenyl molecule: (a, b) electron-induced selective abstraction of iodine from iodobenzene; (c) removal of the iodine atom to a terrace site by lateral manipulation; (d) bringing together two phenyls by lateral manipulation; (e) electron-induced chemical association of the phenyl couple to biphenyl; (f) pulling the synthesized molecule by its front end with the STM tip to confirm the association. Reproduced with permission from ref 137 (http://link.aps.org/abstract/PRL/v85/p2777). Copyright 2000 American Physical Society.

succeeded in combining this single-molecule chemistry with inelastic electron tunneling spectroscopy (IETS) (vibrational spectroscopy) for a precise vibrational identification of the reaction products.[142] The power of this technique is demonstrated by the fact that one can distinguish between the different isotopes, for example, $^{12}C^{16}O$ and $^{13}C^{18}O$. Here the molecules were adsorbed on the Cu(001) and Cu(110) surfaces.[143] Furthermore, excitation of a molecular vibration with electrons from the STM tip can be used to induce motion of a molecule. An illustration of this is the manipulation of an acetylene molecule on Cu(001) at 8 K, where excitation of the C−H stretch mode induces rotation of the molecule on the surface.[144]

The acetylene (HCCH) molecule adsorbed on Cu(001) at 9 K has been dissociated[145] into ethynyl (CCH) and then into dicarbon (CC) species by using the method described in ref 143. Pulses of positive surface voltages in the range 2−3 V have been used to dissociate the molecule. The CCH and CC products of the dissociation have been identified using both STM imaging (Figure 33) and IETS.[146] In this latter case, using HCCD and DCCD isotopes permitted unambiguous assignments of the molecular fragments. Subsequent theoretical calculations have explained why the other modes, namely, the C−C stretch, C−H bend, and molecule surface vibration, are absent.[147−149] The STM-induced dissociations were considered to be related to electronic excitation processes similar to the DIET processes involved in the hydrogen desorption from hydrogenated silicon surfaces (see section 3.1). Similar studies combining STM dissociation and vibrational spectroscopy have been performed to investigate the dehydrogenation of ethylene on Ni(110),[150] pyridine on Cu(001),[151,152] and benzene on Cu(001).[151,152]

Electronic excitation with the STM can also be used to induce bond-making between two molecules or between a molecule and an atom adsorbed on a surface. Two different methods have been illustrated by Ho's group. The first method consists of transferring a molecule from the surface

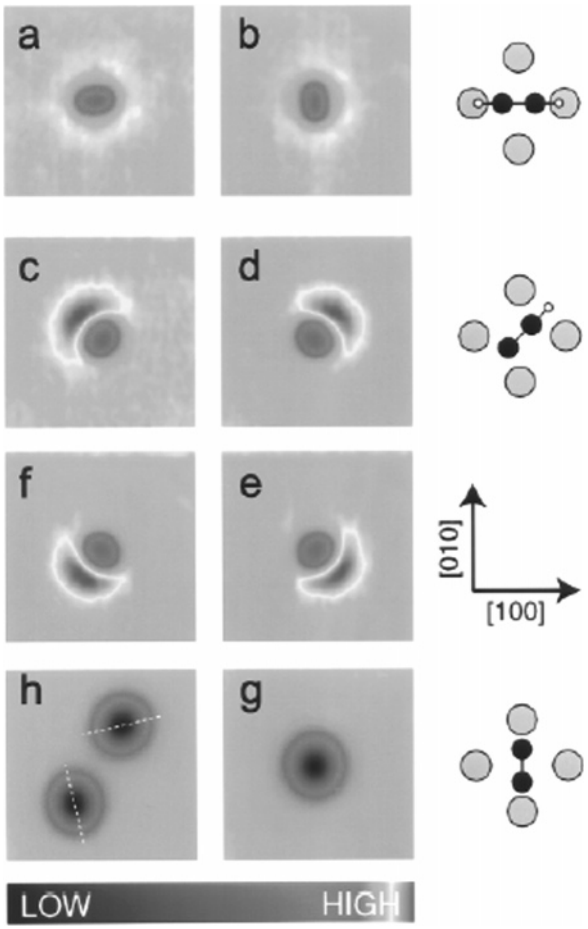

Figure 33. Constant-current STM images (38 × 38 Å^2) of DCCD, CCD, and CC at 9 K on a Cu(001) surface. The vertical range is −1.20 to +0.07 Å. All possible orientations of these molecules on the 4-fold hollow site are shown. Site assignments were confirmed by simultaneously resolving both the molecules and the copper lattice using a tip modified with an adsorbed species and tunneling parameters different from those used for these images. Images of CCH and CCD are nearly identical; CCD is shown because the tip-induced rotation rate of CCH is higher, making imaging difficult. Key: (a, b) DCCD; (c−f) CCD (the image minima are displaced 0.7 Å from the 4-fold hollow site along the (110) axes); (g, h) one and two CC molecules, respectively. Images a−g were taken at 10 pA tunneling current and 50 mV sample bias. Image h was taken during a separate experiment at 10 nA and 100 mV to emphasize the difference in molecular orientation. The directions of the Cu(100) and Cu(010) axes are indicated by the dashed white lines and are rotated 20° with respect to those of the other images. Schematics of the molecular orientation are shown next to the images they represent for (b), (d), and (g). The scale is enlarged 5× with respect to the images. Reproduced with permission from ref 145 (http://link.aps.org/abstract/PRL/v84/p1527). Copyright 2000 American Physical Society.

to the STM tip and then bringing this molecule with the STM tip close to the targeted atom or molecule. The desired bond is then created between the two species by an increased surface voltage and tunnel current.[153] This method has been applied to the formation of Fe(CO) and $Fe(CO)_2$ molecules starting from an Fe atom and two separate CO molecules adsorbed on a Ag(110) surface at 13 K (Figure 34). The produced molecules have been characterized by vibrational spectroscopy using inelastic electron tunneling spectroscopy.[154] The second method has been illustrated by the bonding of a CO molecule with an O atom to produce a CO_2 molecule.[155] The CO molecule was moved close to the O atom on the Ag(110) surface at 13 K by lateral manipula-

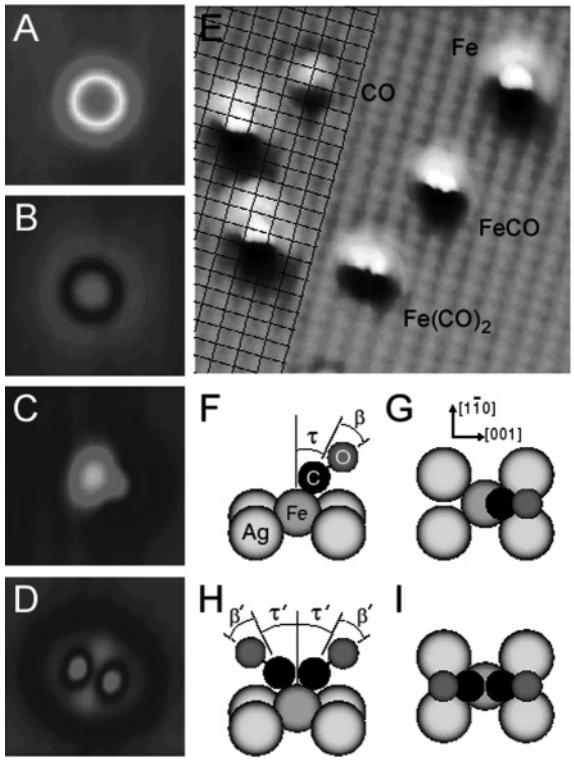

Figure 34. Formation of Fe(CO) and $Fe(CO)_2$ molecules starting from an Fe atom and two separate CO molecules adsorbed on a Ag(110) surface at 13 K. STM topographic images (25×25 Å^2) recorded at 70 mV bias and 0.1 nA without a CO molecule attached to the tip for (A) Fe, (B) CO, (C) Fe(CO), and (D) $Fe(CO)_2$. (E) Atomically resolved STM topographic image recorded at 22 mV bias and 2.5 nA tunneling current with a CO molecule attached to the tip. All species, including CO, image as protrusions. The Fe(CO) image appears similar to that of $Fe(CO)_2$ because of frequent 180° flips during the scan with these tunneling parameters. In this image, it is not the tip height (z) that is displayed but its derivative (dz/dy), where y is the scan direction (from top to bottom). This has the effect of illuminating the scan area from the top of the image and accentuating small corrugations. Therefore, each protrusion shows a bright illuminated side facing the top and a dark shadow facing the bottom. A grid is drawn through the Ag(110) surface atoms to guide the determination of the adsorption sites. (F) The side view and (G) the top view of Fe(CO) show the CO to be tilted by an angle τ and bent by an angle β as suggested by the asymmetry in image C. The 4-fold adsorption site is determined from (E). (H) The side view and (I) the top view of $Fe(CO)_2$ show a similar tilt and bent geometry with angles τ' and β' as implied by images D and E. Reproduced with permission from *Science* (http://www.aaas.org), ref 153. Copyright 1999 American Association for the Advancement of Science.

tion with the STM tip (Figure 35). Then the bonding between the CO molecule and the O atom was induced by tunneling electrons. However, in this latter case, the produced CO_2 molecule desorbs from the surface[155] and cannot be characterized by vibrational spectroscopy.

These studies demonstrate that very detailed investigations of bond-breaking and bond-making chemical reactions are possible at the level of single molecules.[156] A couple of other examples illustrate the potential of this technique. An interesting case is that of NH_3 molecules adsorbed on the Cu(100) surface at 5 K.[157] Careful choice of the tunnel conditions can be used to select either translation of the NH_3 across the surface or desorption of the molecule. Translation of NH_3 is observed for tunnel currents below 0.5 nA, with a threshold voltage at 400 mV. Desorption occurs preferentially at higher tunnel currents >1 nA and at a lower voltage

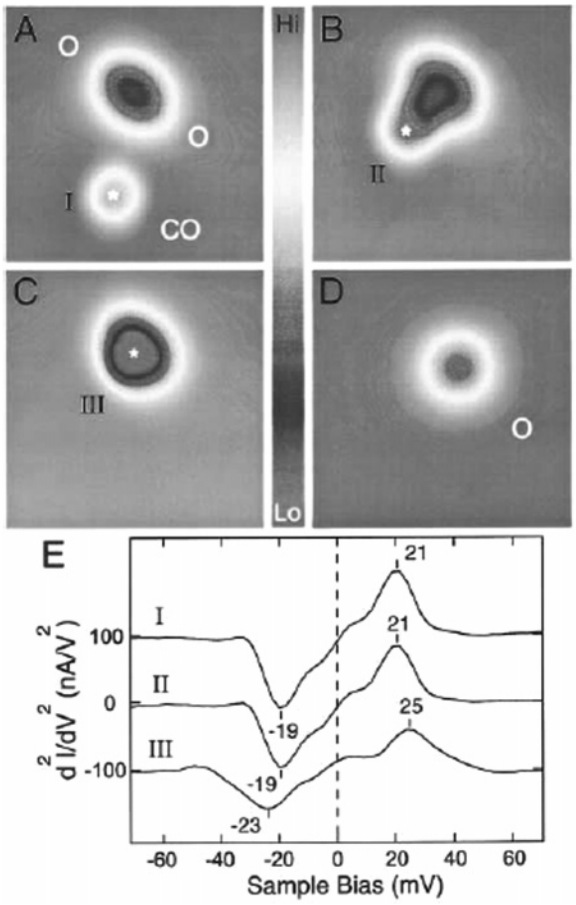

Figure 35. STM topographical images obtained with a bare tip, 70 mV sample bias, and 1 nA tunneling current, showing the manipulation of a CO molecule toward two O atoms coadsorbed on Ag(110) at 13 K and the corresponding vibrational spectra taken over the CO. (A) Single CO molecule and two O atoms. (B) The CO was moved toward the O atoms by applying sample bias pulses (1240 mV) after positioning of the tip over it. This movement prevented the measurement of the C−O stretch (267 meV[153]). (C) The CO was moved to the closest distance from the two O atoms to form the O−CO−O complex. (D) An additional voltage pulse applied to the CO side of the complex led to an image of the remaining O atom on the surface. The scan area of (A)−(D) is 29×29 Å^2. (E) Single-molecule vibrational spectra obtained by STM imaging−IETS for CO at positions marked by asterisks in (A)−(C). The spectra displayed are averages of multiple scans from 270 to 170 mV and back down with subtraction of the background spectra taken over clean Ag(110). A dwell time of 300 ms per 2.5 mV step and 7 mV rms bias modulation at 200 Hz were used for recording the spectra. The line markers indicate the positions of the vibrational features. The energies for these positions were determined by fitting the spectra in the region of a peak or a dip to Gaussian functions. The relative conductance changes, $\Delta\sigma/\sigma$, where $\sigma = dI/dV$, are 9%, 9%, and 5% for the hindered rotation mode at positive sample bias in spectra I, II, and III, respectively. Reproduced with permission from ref 155 (http://link.aps.org/abstract/PRL/v87/p166102). Copyright 2001 American Physical Society.

threshold of 270 mV. These energies correspond to the N−H stretch at the translation threshold and the first overtone of the $N-H_3$ umbrella mode for the desorption threshold. Thus, translation occurs via the excitation of the stretch mode and desorption via excitation of the umbrella mode. The second example is the transformation of *trans*-2-butene into 1,3-butadiene by electron-induced dehydrogenation, which demonstrates that conformational changes can take the form of an isomerization, modifying the chemical nature of the molecule.[158] A description of inelastic electron tunneling

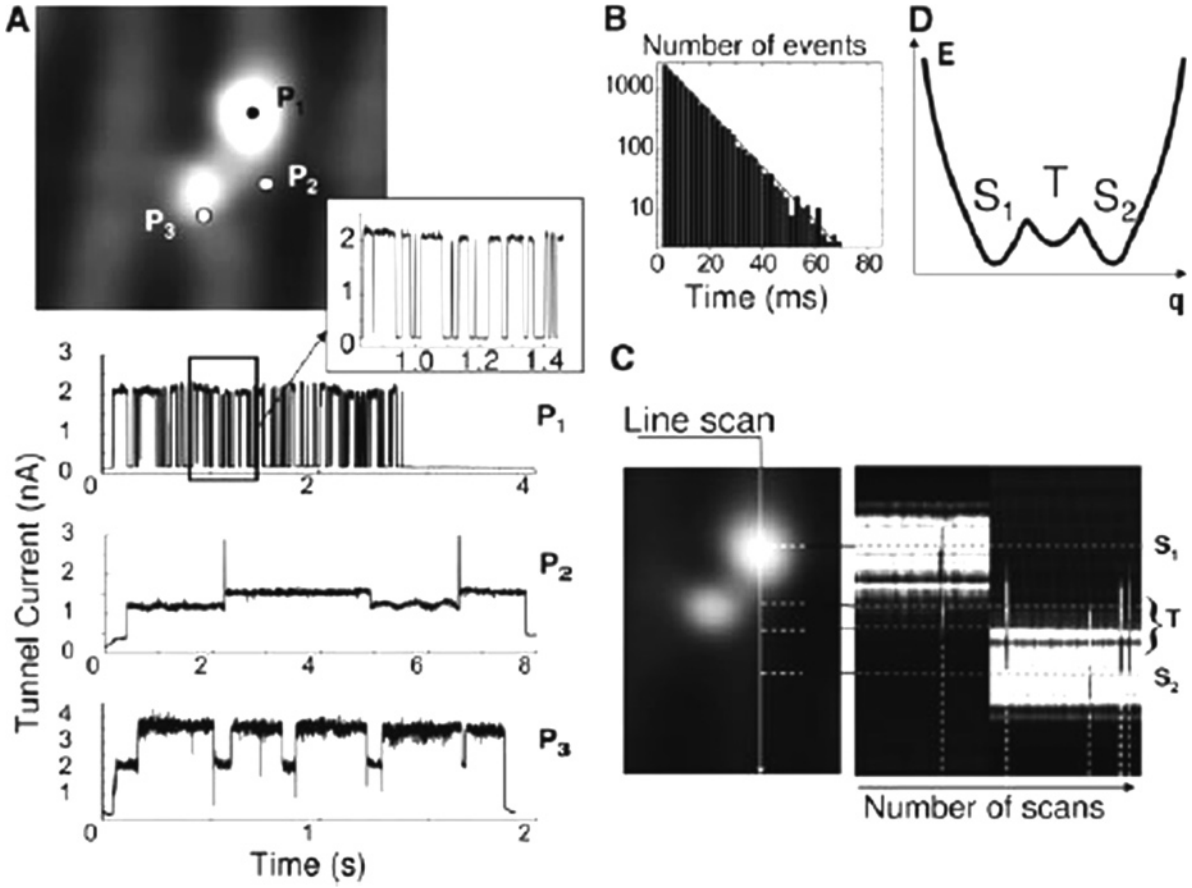

Figure 36. Biphenyl molecules on Si(100)-2×1 at 5 K, a bistable molecule. (A) STM topography (20 × 20 Å^2, $V_S = -2$ V, $I = 0.56$ nA) of a biphenyl molecule. The tunnel current during the surface voltage pulse ($V_S = -2.5$ V, duration 10 s) is shown for three different STM tip positions, P_1, P_2, and P_3. (B) Exponential distribution of the time interval between peaks of the tunnel current curve (P_1) in (A). (C) On the left side, an STM topography of a biphenyl molecule showing the repeatedly scanned line. On the right side, the line scan is shown as a function of time ($V_S = -3$ V, $I = 0.1$ nA). The scan speed is 90 nm/s. The bright features, S_1, T, and S_2, indicate the successive positions of the molecule. (D) Schematic of the ground-state potential energy surface of biphenyl on Si(100). q is an arbitrary reaction coordinate. Reproduced with permission from *Science* (http://www.aaas.org), ref 36. Copyright 2005 American Association for the Advancement of Science.

spectroscopy from a theoretical point of view has been the subject of a recent review.[159]

4.3. Reversible Dynamics in Single Molecules

The STM manipulation by electronic excitation of biphenyl molecules at room temperature led to irreversible molecular movement.[135,136] However, it was realized that the reversible dynamic process of the bistable biphenyl movement could be explored[36] by lowering the substrate temperature. The effect of lowering the temperature is to allow the molecule to be trapped into molecular configurations which would not appear stable at room temperature. As mentioned in section 3.1, electronic excitation induces bond-breaking by delivering a large amount of energy to the molecule, which leads to irreversible dynamic processes. This is especially true for electronic transitions. However, electron (hole) attachment can deliver a smaller amount of energy provided the occupied and unoccupied molecular orbitals lie close in energy to the Fermi level of the surface. A biphenyl molecule adsorbed on a Si(100) surface illustrates this case.[36] Here, the bistable movement of the molecule between two stable configurations (S_1 and S_2) could be activated by hole attachment to occupied π resonances of the adsorbed biphenyl molecule. A positive ion resonance is formed by an electron leaving the molecule, which then relaxes as another electron hops from the substrate to the molecule, similar to that observed in benzene.[131−133] In fact, the dynamical behavior has been found to be very complex. In addition to the two stable (S_1 and S_2) states, a transient (T) state was observed to play an important role (Figure 36). The dynamics of the molecule could be followed in real time (with a limited band-pass of about 1 kHz) by recording the tunnel current during the molecular dynamics. Two separate reversible movements of the molecules ($S_1 \rightarrow S_2$ or $S_1 \rightarrow T$) could be studied in detail. Interestingly, the two different movements of the biphenyl molecule could be selectively activated by choosing either the surface voltage (electron energy) or the localization of the electronic excitation inside the molecule. The size of the biphenyl molecule STM image is about 1 nm, and the spatial resolution of the low-temperature STM can be estimated to be about 0.05 nm. Therefore, it has been possible to explore the effect of the localization of the electronic excitation inside the molecule. The selectivity of the molecular dynamics associated with the localization of the electronic excitation inside the molecule can be explained as follows. The biphenyl molecule possesses various electronic resonances (occupied molecular orbitals) whose energy and spatial localization inside the molecule are different due to the molecular interaction with the surface. Each of these resonances was then locally excited with the STM tip, which demonstrated that each resonance was associated with a given movement of the molecule, i.e., either the $S_1 \rightarrow S_2$ switch

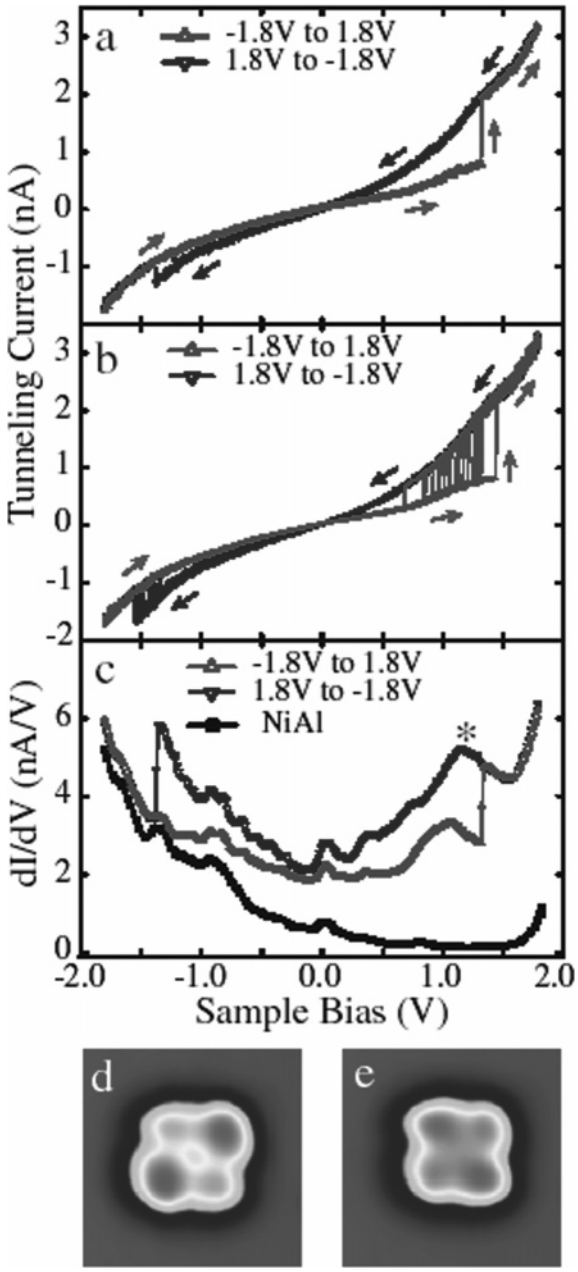

Figure 37. Reversible conformational change of a ZnEtiol molecule on a NiAl(110) surface at 13 K. (a) $I-V$ characteristics of a ZnEtioI molecule. The STM tip was positioned over the center of a molecule in type I conformation. After the feedback was turned off, the sample bias was decreased from the imaging condition (0.7 V) to the beginning of the voltage cycle, −1.8 V. The pair of $I-V$ curves corresponds to variation of the tunneling current as the sample bias was ramped up from −1.8 to +1.8 V and then ramped down from +1.8 to −1.8 V. The voltage step size is 12 mV. (b) A set of 21 pairs of $I-V$ curves recorded consecutively over the molecule, showing variations in the threshold voltages for reversible current jumps. (c) dI/dV spectra recorded simultaneously with the two $I-V$ curves shown in (a), compared to a background spectrum acquired over a clean NiAl(110) surface. The dI/dV curves were recorded by a lock-in amplifier, with an ac modulation of 10 mV rms amplitude added to the sample bias. An electronic state at −1.25 V (*) is evident in spectra taken over the molecule. (d) Image of a molecule in type I-L conformation. (e) Image of a type II-L conformation. Each image size is 33 × 33 Å^2. Reproduced with permission from ref 160 (http://link.aps.org/abstract/PRL/v93/p196806). Copyright 2004 American Physical Society.

or the $S_1 \rightarrow T$ transition. From these results, the localization of the electronic excitation inside the molecule is manifestly a powerful parameter for controlling the dynamics of a single molecule. This demonstration of electronic control of single-molecule dynamics opens new perspectives for artificial molecular nanomachines. A bistable molecule is a very simple prototype of a molecular nanomachine. Indeed, bistability is an interesting molecular function since it can be used in molecular switches, molecular memories, or molecular logic devices.

Another example of a reversible conformational change within a molecule induced by electronic excitation with the STM tip is that of zinc(II) etioporphyrin I (ZnEtioI) molecules adsorbed on a NiAl(110) surface at 13 K.[160] However, the mechanism for switching the molecule is not the same. STM images of these ZnEtioI molecules show the presence of two conformations, a type I conformation where two of the four lobes are distinctly brighter than the other two and a type II conformation where all four lobes have roughly the same intensity. When I(V) spectra were taken of a molecule, abrupt jumps in the current were observed, either at positive voltage when ramping from −1.8 to +1.8 V or at negative voltage when ramping in the other direction from +1.8 to −1.8 V (Figure 37). Subsequent imaging of the molecule showed that it had changed conformation. Averaging over many curves indicated the presence of thresholds at +1.0 V (from I to II) and −1.3 V (from II to I). The threshold at −1.0 V did not depend on the tip−sample separation, whereas the threshold at −1.3 V showed a linear displacement of the threshold toward lower (more negative) voltages as the tip−sample separation was increased. The derivative of the I(V) spectra showed a pronounced peak at about 1.25 V, while no such peak was visible at negative biases. This peak at 1.25 V was attributed to the lowest unoccupied π^* molecular orbital (LUMO) of the molecule. The type I to type II transformation is dominated by a mechanism where an electron from the tip attaches to the molecule, forming a negative ion resonance before inelastically tunneling into a lower electronic state in the substrate. The type II to type I transformation at negative voltage was explained by the electric field acting on the surface dipole formed by the $Zn^{2+}-Ni$ interaction and overcoming the energy barrier for conformational change. The STM allows the surface atoms to be resolved, which reveals that the center of the molecule is over the bridge site along the Ni trough. This places a pair of opposite pyrrole rings over the neighboring Al atoms and the other two rings over the Ni trough. As a consequence the four pyrrole rings experience different interactions with the surface, leading to a nonplanar geometry. This is similar to the distortion found in ligand-coordinated zinc porphyrin molecules.[161]

5. Conclusions

Over the past 15 years, the electronic control of single-molecule dynamics has been tremendously improved. The ability to combine the electronic excitation, the lateral and vertical displacement, and the vibrational spectroscopy of reactants and products has enabled investigation in incredible detail of chemical reactions at the level of individual molecules.[137,139,142,153] Extending these studies to reversible molecular movements has opened up new perspectives for using a single functionalized molecule as a molecular nanomachine. Provided the molecule has been properly designed for having a specific function (bistability, emission of photons, etc.), the electron control offers very flexible methods for powering and controlling the operation of the

molecular nanomachine.[36] Indeed, both the energy and the spatial localization of the electronic excitation inside the molecule can be used as parameters of control.

Many further improvements are in progress for the electronic control of single-molecular dynamics.

(1) Whereas relatively simple molecules have been used so far, more complex molecular architectures having several functions can be fabricated by chemical synthesis, by self-assembly, or by manipulation with the STM. Not only molecules can be used for such assemblies, but also other kinds of nanoobjects such as functionalized nanocrystals.[162,163]

(2) The yields of the electronic processes (probability per electron for producing a given process) which have been studied are relatively small (in the range 10^{-6} to 10^{-10}). Increasing the yield will require a decrease in the electronic coupling between the molecule and the surface. This can be achieved with other methods such as the use of thin insulating layers,[99,164−166] the use of wide-band-gap semiconductors,[167−171] controlled manipulation of passivated semiconductor surfaces,[172−175] or the use of physisorbed rather than chemisorbed species.[176] However, by decreasing the electronic coupling between the molecule and the surface, one may also decrease the adsorption energy of the molecule, which may then diffuse more easily across the surface.

(3) Controlling the electronic processes by excitation with tunneling electrons from the STM tip is made difficult by the complexity of the inelastic tunneling effects. By combining laser excitation with the STM,[95] one can expect to benefit from the advantages of both laser excitation for well-defined electronic excitation and the STM for localized excitation. However, achieving a quantum control of a single molecule on a surface similar to that obtainable on gas-phase molecules is still far from being possible.

In the long term, the principal issue for the electronic control of single-molecular dynamics is the "marriage" between microelectronics and biochemistry. Within the usual molecular electronic schemes, molecules should be used to build either hybrid-molecular or monomolecular devices.[177] However, one can imagine alternative perspectives where "classical" electronic devices connected to individual functionalized molecular nanomachines would separately control their operation. Molecular functions to be controlled in this way could be optical, chemical, or biological functions. Of course, a viable nanomachine should be capable of repetitive motion though not necessarily continuous motion. At present, they lack a permanent source of fuel. This is one problem that needs to be resolved at both a fundamental and application level. Repetitive operation requires a controlled source, which could be electrons or even photons.

6. Acknowledgments

We thank our former Ph.D. students who have contributed to the success of this research work, Franck Rose, Laetitia Soukiassian, Mathieu Lastapis, and Romain Bernard, past postdoctoral students, Marilena Carbone, Kirill Bobrov, Alex Laikhtman, and Marta Martin, and our present Ph.D. students, Marion Cranney, Guillaume Baffou, and Amandine Bellec. This work is also the result of fruitful collaborations with Lucette Hellner, Christian Joachim, Patrick Soukiassian, Alon Hoffman, Maria-Novella Piancastelli, and Philippe Bergonzo. Financial support has been provided by the CNRS and the European Union Network "Atomic and Molecular Manipulation: A New Tool for Science and Technology" (AMMIST).

7. References

(1) Herzberg, G. *Molecular spectra and molecular structure*; Van Nostrand Reinhold Co.: London, 1966.
(2) Porter, G.; Windsor, M. W. *J. Chem. Phys.* **1953**, *21*, 2088.
(3) Gilbert, A.; Baggott, J. *Essentials of molecular photochemistry*; Blackwell Science: Oxford, U.K., 1995.
(4) Berkowitz, J. *Photoabsorption, photoionization and photoelectron spectroscopy*; Academic Press: New York, 1979.
(5) Calvert, J. G.; Pitts, J. N. *Photochemistry*; John Wiley: New York, 1966.
(6) Kunz, C. *Synchrotron radiation*; Springer-Verlag: New York, 1979.
(7) Berry, R. S.; Leach, S. *Adv. Electron. Electron Phys.* **1980**, *57*, 394.
(8) Fournier, P. G.; Comtet, G.; Odom, R. W. *Adv. Mass Spectrosc.* **1977**, *7*, 77.
(9) Los, J.; Govers, T. R. In *Collision Spectroscopy*; Cooks, R. G., Ed.; Plenum: New York, 1978.
(10) De Bruijn, D. P.; Los, J. *Rev. Sci. Instrum.* **1982**, *53*, 1020.
(11) Comtet, G.; Fournier, P.; Lassier-Govers, B. *Chem. Phys.* **1986**, *101*, 299.
(12) Fournier, P. G.; Comtet, G.; Odom, R. W.; Locht, R.; Maas, J. G.; Van Asselt, N. P. F. B.; Los, J. *Chem. Phys. Lett.* **1976**, *40*, 170.
(13) Avouris, Ph.; Gelbart, W. M.; El-Sayed, M. A. *Chem. Rev.* **1977**, *77*, 793.
(14) Leach, S.; Dujardin, G.; Taieb, G. *J. Chim. Phys. Phys.-Chim. Biol.* **1980**, *77*, 705.
(15) Dujardin, G.; Leach, S.; Taieb, G.; Maier, J. P.; Gelbert, W. M. *J. Chem. Phys.* **1980**, *73*, 4987.
(16) Dujardin, G. State Thesis, University of Paris XI, Orsay, France, 1982.
(17) Spears, K. G.; Rice, S. A. *J. Chem. Phys.* **1971**, *55*, 5561.
(18) Gruebele, M.; Bigwood, R. *Int. Rev. Phys. Chem.* **1998**, *17*, 91.
(19) Menzel, D.; Gomer, R. *J. Chem. Phys.* **1964**, *41*, 3311.
(20) Readhead, P. A. *Can. J. Phys.* **1964**, *42*, 886.
(21) Tolk, N. H.; Traum, M. M.; Tully, J. C.; Madey, T. E. *Desorption Induced by Electronic Transitions*; Springer-Verlag: New York, 1983.
(22) Avouris, Ph.; Walkup, R. E. *Annu. Rev. Phys. Chem.* **1989**, *40*, 173.
(23) Treichler, R.; Wurth, W.; Riedl, E.; Feulner, P.; Menzel, D. *Chem. Phys.* **1991**, *153*, 259.
(24) Dujardin, G.; Comtet, G.; Hellner, L.; Hyrayama, T.; Rose, M.; Philippe, L.; Ramage, M. J. *Phys. Rev. Lett.* **1994**, *73*, 1727.
(25) Huels, M. A.; Parenteau, L.; Sanche, L. *J. Chem. Phys.* **1994**, *100*, 3940.
(26) Knotek, M. L.; Feibelman, P. J. *Phys. Rev. Lett.* **1978**, *40*, 969.
(27) Feulner, P.; Menzel, D.; Dai, H. L.; Ho, W. *Laser spectroscopy and photochemistry on metal surfaces*; World Scientific: River Edge, NJ, 1995.
(28) Tanimura, K.; Ueba, H. *Surf. Sci.* **2005**, *593*, 1.
(29) Petek, H.; Ogawa, S. *Prog. Surf. Sci.* **1997**, *56*, 239.
(30) Eigler, D. M.; Schweizer, E. K. *Nature (London)* **1990**, *344*, 524.
(31) Becker, R. S.; Golovchenko, J. A.; Swartzentruber, B. S. *Nature (London)* **1987**, *325*, 419.
(32) Becker, R. S.; Higashi, G. S.; Chabal, Y. J.; Becker, A. J. *Phys. Rev. Lett.* **1990**, *65*, 1917.
(33) Eigler, D. M.; Lutz, C. P.; Rudge, W. E. *Nature (London)* **1991**, *352*, 600.
(34) Dujardin, G.; Walkup, R. E.; Avouris, Ph. *Science* **1992**, *255*, 1232.
(35) Bartels, L.; Meyer, G.; Rieder, K.-H.; Velic, D.; Knoesel, E.; Hotzel, A.; Wolf, M.; Ertl, G. *Phys. Rev. Lett.* **1998**, *80*, 2004.
(36) Lastapis, M.; Martin, M.; Riedel, D.; Hellner, L.; Comtet, G.; Dujardin G. *Science* **2005**, *308*, 1000.
(37) Wu, S. W.; Ogawa, N.; Ho, W. *Science* **2006**, *312*, 1362.
(38) Charron, E.; Giusti-Suzor, A.; Mies, F. H. *J. Chem. Phys.* **1995**, *103*, 7359.
(39) Lang, N. D. *Phys. Rev. Lett.* **2000**, *84*, 979.
(40) Feenstra, R. M. *J. Vac. Sci. Technol., B* **2003**, *21*, 2080.
(41) Lastapis, M.; Riedel, D.; Mayne, A. J.; Bobrov, K.; Dujardin, G. *Low Temp. Phys.* **2003**, *29*, 196.
(42) Feenstra, R. M.; Meyer, G.; Rieder, K.-H. *Phys. Rev. B* **2004**, *69*, 081309.
(43) Feenstra, R. M.; Gaan, S.; Meyer, G.; Rieder, K.-H. *Phys. Rev. B* **2005**, *71*, 125316.
(44) Palmer, R. E.; Rous, P. J. *Rev. Mod. Phys.* **1992**, *64*, 383.
(45) Lyding, J. W.; Shen, T.-C.; Hubacek, J. S.; Tucker, J. R.; Abeln, G. C. *Appl. Phys. Lett.* **1994**, *64*, 2010.
(46) Shen, T.-C.; Wang, C.; Abeln, G. C.; Tucker, J. R.; Lyding, J. W.; Avouris, Ph.; Walkup, R. E. *Science* **1995**, *268*, 1590.
(47) Sakurai, M.; Thirstrup, C.; Nakayama, T.; Aono, A. *Appl. Surf. Sci.* **1997**, *121*, 107.
(48) Stokbro, K.; Hu, B. Y.-K.; Thirstrup, C.; Xie X. C. *Phys. Rev. B* **1998**, *58*, 8038.

(49) Foley, E. T.; Kam, A. F.; Lyding, J. W.; Avouris, Ph. *Phys. Rev. Lett.* **1998**, *80*, 1336.
(50) Thirstrup, C.; Sakurai, M.; Nakayama, T.; Stokbro, K. *Surf. Sci. Lett.* **1999**, *424*, L329.
(51) Soukiassian, L.; Mayne, A. J.; Carbone, M.; Dujardin, G. *Phys. Rev. B* **2003**, *68*, 035303.
(52) Soukiassian, L.; Mayne, A. J.; Carbone, M.; Dujardin, G. *Surf. Sci.* **2003**, *528*, 121.
(53) Dujardin, G.; Rose, F.; Tribollet, J.; Mayne, A. J. *Phys. Rev. B* **2001**, *63*, 081305.
(54) Dujardin, G.; Rose, F.; Mayne, A. J. *Phys. Rev. B* **2001**, *63*, 235414.
(55) Mayne, A. J.; Rose, F.; Dujardin, G. *Faraday Discuss.* **2000**, *117*, 241.
(56) Dujardin, G.; Mayne, A. J.; Rose, F. *Phys. Rev. Lett.* **2002**, *89*, 036802.
(57) Avouris, Ph.; Walkup, R. E.; Rossi, A. R.; Akati, H. C.; Nordlander, P.; Shen, T.-C.; Abeln, G. C.; Lyding, J. W. *Surf. Sci.* **1996**, *363*, 368.
(58) Avouris, Ph.; Walkup, R. E.; Rossi, A. R.; Chen, T.-C.; Abeln, G. C.; Tucker, J. R.; Lyding, J. W. *Chem. Phys. Lett.* **1996**, *257*, 148.
(59) Salam, G. P.; Persson, M.; Palmer, R. E. *Phys. Rev. B* **1994**, *49*, 10655.
(60) Gao, S.; Persson, M.; Lundqvist, B. I. *Phys. Rev. B* **1997**, *55*, 4825.
(61) Guyot-Sionnest, P.; Li, P. H.; Miller, E. M. *J. Chem. Phys.* **1995**, *102*, 4269.
(62) Soukiassian, L. Ph.D. Thesis, University of Paris XI, Orsay, France, 2002.
(63) Klistner, T.; Nelson, J. *Phys. Rev. Lett.* **1991**, *67*, 3800.
(64) Wintterlin, J.; Avouris, Ph. *J. Chem. Phys.* **1994**, *100*, 687.
(65) Bringans, R. D.; Höchst, H. *Phys. Rev. B* **1982**, *25*, 1081.
(66) Surnev, L.; Tikhov, M. *Surf. Sci.* **1984**, *138*, 40.
(67) Knoesel, E.; Hertel, T.; Wolf, M.; Ertl, G. *Chem. Phys. Lett.* **1995**, *249*, 409.
(68) Martel, R.; Avouris, Ph.; Lyo, I.-W. *Science* **1996**, *272*, 385.
(69) Schubert, B.; Avouris, Ph.; Hoffmann, R. *J. Chem. Phys.* **1993**, *98*, 7593.
(70) Dujardin, G.; Mayne, A. J.; Comtet, G.; Hellner, L.; Le Goff, E.; Jamet, M.; Millet, P. *Phys. Rev. Lett.* **1996**, *76*, 3782.
(71) Hwang, I.-S.; Lo, R.-L.; Tsong, T. T. *Phys. Rev. Lett.* **1997**, *78*, 4797.
(72) Mayne, A. J.; Rose, F.; Comtet, G.; Hellner, L.; Dujardin, G. *Surf. Sci.* **2003**, *528*, 132.
(73) Sakamoto, K.; Jemander, S. T.; Hansson, G. V.; Uhrberg, R. I. G. *Phys. Rev. B* **2002**, *65*, 155305.
(74) Comtet, G.; Hellner, L.; Dujardin, G.; Bobrov, K. *Phys. Rev. B* **2002**, *65*, 035315.
(75) Comtet, G.; Dujardin, G. *Surf. Sci.* **2005**, *593*, 256.
(76) Kim, K.-Y.; Shin, T.-H.; Han, S.-H.; Kang, H. *Phys. Rev. Lett.* **1999**, *82*, 1329.
(77) Lee, S.-H.; Kang, M.-H. *Phys. Rev. Lett.* **1999**, *82*, 968.
(78) Lee, S.-H.; Kang, M.-H. *Phys. Rev. Lett.* **2000**, *84*, 1724.
(79) Matsui, F.; Yeom, H. W.; Amemiya, K.; Tono, K.; Ohta, T. *Phys. Rev. Lett.* **2000**, *85*, 630.
(80) Stipe, B. C.; Rezaei, M. A.; Ho, W. *Phys. Rev. Lett.* **1997**, *79*, 4397.
(81) Schlüter, M.; Cohen, M. L. *Phys. Rev. B* **1978**, *17*, 716.
(82) Brockhouse, B. N. *Phys. Rev. Lett.* **1959**, *2*, 256.
(83) Qiu, X. H.; Nazin, G. V.; Ho, W. *Science* **2003**, *299*, 542.
(84) Hoffmann, G.; Kliewer, J.; Berndt, R. *Phys. Rev. Lett.* **2001**, *87*, 176803.
(85) Aizpurua, J.; Apell, S. P.; Berndt, R. *Phys. Rev. B* **2000**, *62*, 2065.
(86) Meguro, K.; Sakamoto, K.; Arafune, B.; Satoh, M.; Ushioda, S. *Phys. Rev. B* **2002**, *65*, 165405.
(87) Stokbro, K.; Thirstrup, C.; Sakurai, M.; Quaade, U.; Hu, B. Y.-K.; Perez-Murano, F.; Grey, F. *Phys. Rev. Lett.* **1998**, *80*, 2618.
(88) Comtet, G.; Dujardin, G.; Hellner, L.; Lastapis, M.; Martin, M.; Mayne, A. J.; Riedel, D. *Philos. Trans. R. Soc. London, A* **2004**, *362*, 1217.
(89) Guyot-Sionnest, P.; Dumas, P.; Chabal, Y. J.; Higashi, G. S. *Phys. Rev. Lett.* **1990**, *64*, 2156.
(90) Head-Gordon, M.; Tully, J. *J. Chem. Phys.* **1992**, *96*, 3939.
(91) Uchida, H.; Huang, D.; Grey, F.; Aono, M. *Phys. Rev. Lett.* **1993**, *70*, 2040.
(92) Vondrak, T.; Zhu, X.-Y. *Phys. Rev. Lett.* **1999**, *82*, 1967.
(93) Vondrak, T.; Zhu, X.-Y. *J. Phys. Chem.* **1999**, *103*, 4892.
(94) Jing, Z.; Whitten, J. L. *Phys. Rev. B* **1992**, *46*, 9544.
(95) Riedel, D.; Mayne, A. J.; Dujardin, G. *Phys. Rev. B* **2005**, *72*, 233304.
(96) Riedel, D.; Mayne, A. J.; Dujardin, G. *J. Phys. IV* **2005**, *127*, 151.
(97) Herrero, C. P.; Stutzmann, M.; Breitschwerdt, A. *Phys. Rev. B* **1991**, *43*, 1555.
(98) Huang, L. J.; Lau, W. M. *J. Vac. Sci. Technol., A* **1992**, *10*, 812.
(99) Ćavar, E.; Blüm, M.-C.; Pivetta, M.; Patthey, F.; Chergui, M.; Schneider, W.-D. *Phys. Rev. Lett.* **2005**, *95*, 196102.
(100) Lof, R. W.; van Veenendaal, M. A.; Koopmans, B.; Jonkman, H. T.; Sawatzky, G. A. *Phys. Rev. Lett.* **1992**, *68*, 3924.
(101) Wu, S. W.; Nazin, G. V.; Chen, X.; Qiu, X. H.; Ho W. *Phys. Rev. Lett.* **2004**, *93*, 236802.
(102) Sassara, A.; Zerza, G.; Chergui, M. *J. Phys. B* **1996**, *29*, 4997.
(103) Sassara, A.; Zerza, G.; Chergui, M.; Orlandi, G.; Negri, F. *J. Chem. Phys.* **1997**, *107*, 8731.
(104) Orlandi, G.; Negri, F. *Photochem. Photobiol. Sci.* **2002**, *1*, 289.
(105) Persson, B. N. J.; Baratoff, A. *Phys. Rev. Lett.* **1992**, *68*, 3224.
(106) Johansson, P.; Monreal, R.; Apell, P. *Phys. Rev. B* **1990**, *42*, 9210.
(107) Uehara, Y.; Kimura, Y.; Ushioda, S.; Takeuchi, K. *Jpn. J. Appl. Phys.* **1992**, *31*, 2465.
(108) Gimzewski, J. K.; Reihl, B.; Coombs, J. H.; Schlittler, R. R. *Z. Phys. B* **1988**, *72*, 497.
(109) Berndt, R.; Gaisch, R.; Gimzewski, J. K.; Reihl, B.; Coombs, J. H.; Schlittler, R. R.; Schneider, W. D.; Tschudy, M. *Science* **1993**, *262*, 1425.
(110) Thirstrup, C.; Sakurai, M.; Stokbro, K.; Aono, M. *Phys. Rev. Lett.* **1999**, *82*, 1241.
(111) Sakurai, M.; Thirstrup, C.; Aono, M. *Surf. Sci.* **2003**, *526*, L123.
(112) Betzig, E.; Trautman, J. K. *Science* **1992**, *257*, 189.
(113) Moerner, W. E.; Orrit, M. *Science* **1999**, *283*, 1670.
(114) Tsong, T. T. *Phys. Rev. B* **1991**, *44*, 13703.
(115) Lyo, I.-W.; Avouris, Ph. *Science* **1991**, *253*, 173.
(116) Salling, C. T.; Lagally, M. G. *Science* **1994**, *265*, 502.
(117) Dujardin, G.; Mayne, A. J.; Rose, F.; Robert, O.; Tang, H.; Joachim, C. *Phys. Rev. Lett.* **1998**, *80*, 3085.
(118) Sloan, P. A.; Palmer, R. E. *Nature (London)* **2005**, *434*, 367.
(119) Lu, P. H.; Polanyi, J. C.; Rogers, D. *J. Chem. Phys.* **1999**, *111*, 9905.
(120) Sloan, P. A.; Hedouin, M. F. G.; Palmer, R. E.; Persson, M. *Phys. Rev. Lett.* **2003**, *91*, 118301.
(121) Skalicky, T.; Chollet, C.; Pasquier, N.; Allan, M. *Phys. Chem. Chem. Phys.* **2002**, *4*, 3583.
(122) Sloan, P. A.; Palmer, R. E. *Nano Lett.* **2005**, *5*, 835.
(123) Palmer, R. E. *Prog. Surf. Sci.* **1992**, *41*, 51.
(124) Dixon-Warren, St-J.; Jensen, E. T.; Polanyi, J. C. *Phys. Rev. Lett.* **1991**, *67*, 2395.
(125) Cao, Y.; Deng, J. F.; Xu, G. Q. *J. Chem. Phys.* **2000**, *112*, 4759.
(126) Li, Z.-H.; Li, Y.-C.; Wang, W.-N.; Cao, Y.; Fan, K.-N. *J. Phys. Chem. B* **2004**, *108*, 14049.
(127) Self, K. W.; Pelzel, R. I.; Owen, J. H. G.; Yan, C.; Widdra, W.; Weinberg, W. H. *J. Vac. Sci. Technol., A* **1998**, *16*, 1031.
(128) Lopinski, G. P.; Moffat, D. J.; Wolkow, R. A. *Chem. Phys. Lett.* **1998**, *282*, 305.
(129) Lopinski, G. P.; Fortier, T. M.; G.; Moffat, D. J.; Wolkow, R. A. *J. Vac. Sci. Technol., A* **1998**, *16*, 1037.
(130) Gorkhale, S.; Trischberger, T.; Menzel, D.; Widdra, W.; Dröge, H.; Steinrück, H.-P.; Birkenheuer, U.; Gutdeutsch, U.; Rösch, N. *J. Chem. Phys.* **1998**, *108*, 5554.
(131) Kong, M. J.; Teplyakov, A. V.; Lyubovitsky, J. G.; Bent, S. F. *Surf. Sci.* **1998**, *411*, 286.
(132) Patitsas, S. N.; Lopinski, G. P.; Hul'ko, O.; Moffat, D. J.; Wolkow, R. A. *Surf. Sci. Lett.* **2000**, *457*, L425.
(133) Alavi, S.; Rousseau, R.; Patitsas, S. N.; Lopinski, G. P.; Wolkow, R. A.; Seideman, T. *Phys. Rev. Lett.* **2000**, *85*, 5372.
(134) Soukiassian, L.; Mayne, A. J.; Baffou, G.; Comtet, G.; Hellner, L.; Dujardin, G.; Gourdon, A. *J. Chem. Phys.* **2005**, *122*, 134704.
(135) Mayne, A. J.; Lastapis, M.; Baffou, G.; Soukiassian, L.; Comtet, G.; Hellner, L.; Dujardin, G. *Phys. Rev. B* **2004**, *69*, 045409.
(136) Cranney, M.; Mayne, A. J.; Comtet, G.; Dujardin, G. *Surf. Sci.* **2005**, *593*, 139.
(137) Hla, S.-W.; Bartels, L.; Meyer, G.; Rieder, K.-H. *Phys. Rev. Lett.* **2000**, *85*, 2777.
(138) Ullmann, F.; Meyer, G. M.; Loewenthal, O.; Gilli, O. *Justus Liebigs Ann. Chim.* **1904**, *331*, 38.
(139) Bartels, L.; Meyer, G.; Rieder, K.-H. *Phys. Rev. Lett.* **1997**, *79*, 697.
(140) Meyer, G.; Zöphel, S.; Rieder, K.-H. *Appl. Phys. A: Mater. Sci. Process.* **1996**, *63*, 557.
(141) Meyer, G.; Zöphel, S.; Rieder, K.-H. *Phys. Rev. Lett.* **1996**, *77*, 2113.
(142) Stipe, B. C.; Rezaei, M.; Ho, W. *Science* **1998**, *280*, 1732.
(143) Lauhon, L. J.; Ho, W. *Phys. Rev. B* **1999**, *60*, R8525.
(144) Stipe, B. C.; Rezaei, M. A.; Ho, W. *Phys. Rev. Lett.* **1998**, *81*, 1263.
(145) Lauhon, L. J.; Ho, W. *Phys. Rev. Lett.* **2000**, *84*, 1527.
(146) Stipe, B. C.; Rezaei, M.; Ho, W. *Phys. Rev. Lett.* **1999**, *82*, 1724.
(147) Mingo, N.; Makoshi, K. *Phys. Rev. Lett.* **2000**, *84*, 3694.
(148) Lorente, N.; Persson, M. *Phys. Rev. Lett.* **2000**, *85*, 2997.
(149) Lorente, N.; Persson, M.; Lauhon, L. J.; Ho, W. *Phys. Rev. Lett.* **2001**, *86*, 2593.
(150) Gaudioso, J.; Lee, H. J.; Ho, W. *J. Am. Chem. Soc.* **1999**, *121*, 8479.
(151) Lauhon, L. J.; Ho, W. *J. Phys. Chem. A* **2000**, *104*, 2463.
(152) Lauhon, L. J.; Ho, W. *Surf. Sci.* **2000**, *451*, 219.
(153) Lee, H. J.; Ho, W. *Science* **1999**, *286*, 1719.
(154) Lee, H. J.; Ho, W. *Phys. Rev. B* **2000**, *61*, R16347.
(155) Hahn, J. R.; Ho, W. *Phys. Rev. Lett.* **2001**, *87*, 166102.
(156) Ho, W. *J. Chem. Phys.* **2002**, *117*, 11033.

(157) Pascual, J. I.; Lorente, N.; Song, Z.; Conrad, H.; Rust, H.-P. *Nature (London)* **2003**, *423*, 525.
(158) Kim, Y.; Komeda, T.; Kawai, M. *Phys. Rev. Lett.* **2002**, *89*, 126104.
(159) Lorente, N.; Rurali, R.; Tang, H. *J. Phys.: Condens. Matter* **2005**, *17*, S1049.
(160) Qiu, X. H.; Nazin, G. V.; Ho, W. *Phys. Rev. Lett.* **2004**, *93*, 196806.
(161) Shelnutt, J. A.; Song, X.-Z.; Ma, J.-G.; Jia, S.-L.; Jentzen, W.; Medforth, C. J. *Chem. Soc. Rev.* **1998**, *27*, 31.
(162) Bernard, R.; Comtet, G.; Dujardin, G.; Huc, V.; Mayne, A. J. *Appl. Phys. Lett.* **2005**, *87*, 053114.
(163) Bernard, R.; Huc, V.; Reiss, P.; Chandezon, F.; Jegou, P.; Palaçin, S.; Dujardin, G.; Comtet, G. *J. Phys.: Condens. Matter* **2004**, *16*, 7565.
(164) Repp, J.; Meyer, G.; Olsson, F. E.; Persson, M. *Science* **2004**, *305*, 493.
(165) Repp, J.; Meyer, G.; Paavilainen, S.; Olsson, F. E.; Persson, M. *Phys. Rev. Lett.* **2005**, *95*, 225503.
(166) Repp, J.; Meyer, G.; Paavilainen, S.; Olsson, F. E.; Persson, M. *Science* **2006**, *312*, 1196.
(167) Bobrov, K.; Mayne, A. J.; Dujardin, G. *Nature (London)* **2001**, *413*, 616.
(168) Bobrov, K.; Soukiassian, L.; Mayne, A. J.; Dujardin, G.; Hoffman, A. *Phys. Rev. B* **2002**, *66*, 195403.
(169) Bobrov, K.; Mayne, A. J.; Comtet, G.; Dujardin, G.; Hellner, L.; Hoffman, A. *Phys. Rev. B* **2003**, *68*, 195416.
(170) Hellner, L.; Mayne, A. J.; Bernard, R.; Dujardin, G. *Diamond Relat. Mater.* **2005**, *14*, 1529.
(171) Laikhtman, A.; Baffou, G.; Mayne, A. J.; Dujardin, G. *J. Phys.: Condens. Matter* **2005**, *17*, 4015.
(172) Hersam, M. C.; Guisinger, N. P.; Lyding, J. W. *Nanotechnology* **2000**, *11*, 70.
(173) Mayne, A. J.; Soukiassian, L.; Commaux, N.; Comtet, G.; Dujardin, G. *Appl. Phys. Lett.* **2004**, *85*, 5379.
(174) Lopinski, G. P.; Wayner, D. D. M.; Wolkow, R. A. *Nature (London)* **2000**, *406*, 48.
(175) Piva, P. G.; DiLabio, G. A.; Pitters, J. L.; Zikovsky, J.; Rezeq, M.; Dogel, S.; Hofer, W. A.; Wolkow, R. A. *Nature (London)* **2005**, *435*, 658.
(176) Carbone, M.; Piancastelli, M. N.; Casaletto, M. P.; Zanoni, R.; Besnard-Ramage, M. J.; Comtet, G.; Dujardin, G.; Hellner, L. *J. Phys.: Condens. Matter* **2003**, *15*, L327.
(177) Joachim, C.; Gimzewski, J. K.; Aviram, A. *Nature (London)* **2000**, *408*, 541.

CR050177H